

# Erasure conversion in Majorana qubits via local quasiparticle detection

Abhijeet Alase,<sup>1,2</sup> Kevin D. Stubbs,<sup>3</sup> Barry C. Sanders,<sup>1</sup> and David L. Feder<sup>1</sup>

<sup>1</sup>*Institute for Quantum Science and Technology, University of Calgary,  
2500 University Drive NW, Calgary, Alberta T2N 1N4, Canada*

<sup>2</sup>*Centre for Engineered Quantum Systems, School of Physics,  
University of Sydney, Sydney, New South Wales 2006, Australia*

<sup>3</sup>*Department of Mathematics, University of California, Berkeley, California 94720 USA*

Quasiparticle poisoning errors in Majorana-based qubits are not suppressed by the underlying topological properties, which undermines the usefulness of this proposed platform. This work tackles the errors originating from intrinsically excited quasiparticles by developing an erasure conversion scheme based on local quasiparticle detection. To model such measurements, we begin by constructing the quasiparticle position operator for the Kitaev chain. A measurement probe coupling to this operator is shown to allow projective measurements in the Wannier quasiparticle basis. Detection of quasiparticles in a region of width  $d$  adjacent to each Majorana zero-energy mode allows implementation of an error-detecting Majorana stabilizer code  $\mathcal{C}_d$  based on microscopic fermionic (non-topological) physical degrees of freedom. The implementation of  $\mathcal{C}_d$  converts a large fraction of Pauli errors to erasure errors, thus achieving ‘erasure conversion’ in Majorana qubits. We show that the fraction of Pauli errors escaping conversion to erasure errors is exponentially small in  $d$ , a result tied to the exponential localization of Wannier functions which we prove rigorously. The suppression in Pauli error rate comes at the cost of the erasure rate increasing sublinearly with  $d$ , but this can be readily compensated for by a suitable outer code, with the net effect being a higher threshold rate of quasiparticle poisoning. The framework developed here serves as a basis for understanding how realistic measurements, such as conductance measurements, could be utilized for achieving fault tolerance in these systems.

## I. INTRODUCTION

Perhaps the biggest challenge to realizing fault-tolerant quantum computers is suppressing error rates in gate operations to below the thresholds dictated by state-of-the-art error-correcting codes. This was the main attraction of topological qubits from the point of view of fault-tolerant quantum computation [1]: topological qubits provide a route to suppress errors at the hardware level. Information in topological qubits is encoded non-locally in low-energy anyonic excitations [2, 3]. Therefore, only non-local errors can alter the state of the stored qubit, thus suppressing Pauli errors. Whereas local errors can transfer population from the topologically degenerate ground states to higher energy excited states causing leakage, these processes are suppressed by constant bulk energy gap. At equilibrium, the density of excited higher-energy quasiparticles (QPs) is exponentially small in the ratio of the bulk energy gap to the absolute temperature [1].

The field of topological quantum computation began with the hope that one might be able to perform arbitrarily long computations without requiring active error correction [2, 4]. However, the topological systems that are currently in contention for being used as topological qubits lack self error-correcting properties [5], because they allow propagation of anyonic excitations at a constant energy cost [6, 7]. Topological qubits decohere due to the interactions between a computational anyon and excited-state QPs, a process called QP poisoning. Whereas the density of higher-energy QPs is exponentially small in the bulk gap at thermal equilibrium, they

can arise during non-adiabatic gate operations [8]. Classical noise sources at characteristic frequencies close to the bulk gap can also lead to an increased density of QPs [9]. Unlike the errors that originate from finite overlap of computational anyons, the QP poisoning errors cannot be suppressed by simply increasing the distance between computational anyons. Therefore, QP poisoning errors in topological qubits must be addressed using other approaches.

Majorana-based qubits are leading candidates for topological qubits [10]. Such a qubit can be realized on a tetron device, comprising a pair of semiconducting nanowires with strong spin-orbit coupling in close proximity to a superconductor [4, 5, 9]. A tetron device hosts four spatially separated Majorana zero-energy modes (MZMs), and therefore has four degenerate ground states. A qubit is conventionally encoded in the two even-parity ground states of a tetron, and all logical operators are products of two out of the four MZMs hosted by the tetron. Since all four MZMs are spatially separated, the rates of logical Pauli errors are suppressed exponentially in the length of the nanowires as long as the noise processes are local [11]. Even-parity local noise processes can generally excite QPs, however. Sources of such noise processes include charge noise, thermal noise, and non-adiabatic gate operations [11]. The interaction of MZMs with these QPs, namely QP poisoning, leads to decoherence of the qubit stored in MZMs. As these even-parity processes can occur without any exchange of electrons with the environment, we refer to them as intrinsic QP poisoning processes to distinguish them from extrinsic QP poisoning caused by interactions with the

environment [12]. Mitigating the influence of these intrinsic QPs is the focus of the current work.

QP poisoning errors can be corrected, in general, by implementing conventional error-correcting codes [13]. Specialized error-correcting codes that use computational anyons as physical degrees of freedom to store logical qubits have also been explored [14]. Examples of such codes include Majorana surface codes [15, 16], which belong to the larger family of Majorana fermion codes [17]. However, achieving fault-tolerance with any error-correcting code requires physical error rates to be below a certain threshold value, a condition that topological qubits with high rates of QP poisoning may not meet. Moreover, the resources required for error correction depend crucially on physical error rates. For these reasons, strategies that further suppress the error rates at the hardware level are highly desirable.

In principle, given total control over the microscopic fermionic degrees of freedom, the local QP poisoning errors in a Majorana qubit are expected to be detectable and correctable, for reasons that are reviewed in §IID. Yet, a high level of control over microscopic degrees of freedom is experimentally challenging in these systems, and would seem to defeat the purpose of using topological qubits in the first place. The problem addressed in this work is how to tackle QP poisoning errors with minimal access to the microscopic degrees of freedom.

Towards this goal, we explore the possibility of erasure conversion in Majorana qubits. Erasure conversion is the process of converting Pauli errors to erasure errors. This technique has already been demonstrated to be effective in some non-topological qubit platforms [18–21]. An error process is convertible to erasure if it leaves a signature that can be detected without disturbing the qubit. In Majorana qubits, intrinsic QP poisoning processes in fact do leave such a signature. Consider a pair of QPs excited in a topological wire, one of which is absorbed by a computational anyon, causing a QP poisoning error. This leaves behind a QP excitation in the bulk of the wire away from the MZMs. Detection of this QP without affecting the stored qubit should be possible, because the qubit is stored in MZMs whereas the QP resides in the bulk of the wire. The QPs that are excited near the ends of the wire are more likely to poison the MZMs than those excited away from the ends, so a local detection of QPs should be much more effective than a position non-resolving detection scheme for the purpose of erasure conversion.

There are three main challenges to formalizing this strategy. The first and most important is to model the local detection of QPs. In the Kitaev tetron model of a Majorana qubit the description of QPs is readily available, as the Hamiltonian is quadratic and diagonalizable via a Bogoliubov transformation. However, these QPs are not localized except at the fixed point parameter values. To define local QP measurements, we first construct a QP position operator that satisfies certain desiderata. The eigenstates of the QP position operator describe Wan-

nier QPs [22], which we prove are exponentially localized throughout the topological phase. This localization property is crucial to achieving high levels of suppression of Pauli errors. Local QP detection is then defined as a projective measurement in the basis of Wannier QPs.

Having modeled the QP detectors, the next task is to devise an erasure conversion scheme based on QP detection. In this work, we make a crucial observation that an erasure conversion scheme is equivalent to implementing an error-detecting code at the hardware level, and construct some simple error-detecting Majorana stabilizer codes that can be implemented with QP detectors. The first application is to the fixed-point parameter values of the Kitaev tetron, as the ground states at these parameter values are known to form a Majorana fermionic stabilizer code [17]. We show that the stabilizers of this code are in fact the Wannier QP parity operators. This observation allows for the design of error-detecting codes for encoding a single qubit in the physical fermionic degrees of freedom of the Kitaev tetron throughout the topological phase, such that any local parity-preserving error taking the system out of the code space can be detected by QP measurement. More concretely, we construct a family of codes  $\{\mathcal{C}_d\}$  parametrized by a non-negative integer  $d < n/2$ , where  $n$  is the length of each chain in Kitaev tetron. Effectively, our erasure conversion scheme has a tunable integer parameter  $d$ . The even-parity distance of each code  $\mathcal{C}_d$  is  $4d + 4$ . We show that a QP detector with inverse resolution  $\lambda$  enables implementation of the codes  $\{\mathcal{C}_d, \lambda \leq d\}$ , where  $\mathcal{C}_0$  is identical to the conventional encoding of the qubit in a tetron at the fixed point. Wannier function-based error-detecting codes in this work are conceptually similar to the smeared stabilizer codes investigated in Ref. [23].

There are some key differences between the aforementioned error-detection codes and other Majorana codes in the literature, such as the Majorana surface code. The physical degrees of freedom in our codes are MZMs as well as the bulk fermion modes in the tetron, which permits the implementation of error-detection codes on a single Majorana tetron via QP detection. In contrast, for most Majorana codes the physical degrees of freedom are MZMs hosted by constituent tetrtons/hexons, implemented on a network comprising multiple tetrtons or hexons, which do not require QP detection but rather joint parity measurements involving multiple MZMs. We emphasize that the error-detecting codes in this work do not provide a substitute for higher-level Majorana codes; rather, they are envisaged as forming a lower layer of error correction on which other (erasure-tolerant) codes can be concatenated, as is the case for erasure conversion schemes for other qubit platforms.

To assess the performance of the erasure conversion scheme, this work considers a simple model of intrinsic QP poisoning. We show that the fraction of Pauli errors escaping conversion to erasure errors is exponentially small in  $d$ . On the other hand, the erasure errors increase sublinearly in  $d$ . Erasure errors are known to be easier to

correct than Pauli errors [24, 25]. This is evident from the fact that some quantum error correction codes achieve threshold erasure rates of 50% per QEC cycle, whereas the threshold Pauli error rates are usually on the order of 1%. Consequently, QP detection allows fault-tolerant computation for significantly higher value of QP poisoning rates compared to no QP detection. Moreover, this implies a significant reduction in resources required for implementing error correction.

The organization of this manuscript is follows. In §II, the relevant properties of the Kitaev tetron are reviewed. A model of QP detector with finite spatial resolution is constructed in §III. In §IV, we design Majorana error-detecting codes that can be implemented with the help of QP detectors. These codes provide a rigorous description of the erasure conversion scheme. The performance of our erasure conversion scheme is assessed in §V. Finally, the results are summarized and open questions are discussed in §VI.

## II. BACKGROUND

In this section, we review the theory of quadratic number non-conserving fermionic Hamiltonians, and the Kitaev chain model of a one-dimensional topological superconductor and its error-correcting properties. We also briefly review some tools from the covariance matrix framework.

### A. Quadratic fermionic operators

Let  $a_j$  and  $a_j^\dagger$ ,  $j = 1, \dots, n$ , be fermionic annihilation and creation operators respectively on the Fock space  $\mathcal{F}_n$ . They satisfy the canonical anticommutation relations

$$[a_j, a_{j'}^\dagger]_+ = \delta_{jj'}, \quad [a_j, a_{j'}]_+ = 0, \quad (1)$$

where  $[\bullet, \bullet]_+$  denotes the anticommutator. The fermion-number and total-parity operators are defined to be  $\hat{N} = \sum_j a_j^\dagger a_j$  and  $(-1)^{\hat{N}}$  respectively. A quadratic fermionic Hermitian operator  $\hat{A}$  can be expressed as [26]

$$\hat{A} = \frac{1}{2} \Phi^\dagger A \Phi + \text{constant}, \quad (2)$$

where  $\Phi^\dagger = [a_1^\dagger \dots a_n^\dagger \ a_1 \dots a_n]$  and  $A$  is the Bogoliubov de-Gennes (BdG) matrix. The size of  $A$  is  $2n \times 2n$  and we denote its entries by  $A_{jm, j'm'}$ , where  $j, j' \in 1, \dots, n$  and  $m, m' \in \{1, 2\}$ . Such an operator is not necessarily number conserving, i.e.,  $[\hat{A}, \hat{N}]_- \neq 0$ , where  $[\bullet, \bullet]_-$  denotes the commutator. However,  $\hat{A}$  conserves the total parity, i.e.,  $[\hat{A}, (-1)^{\hat{N}}]_- = 0$ . The BdG matrix  $A$  represents the action of commutator of  $\hat{A}$  with linear fermionic

operators, i.e.

$$\begin{aligned} [\hat{A}, a_j^\dagger]_- &= \sum_{j'=1}^n \left( A_{j1, j'1} a_{j'}^\dagger + A_{j1, j'2} a_{j'} \right), \\ [\hat{A}, a_j]_- &= \sum_{j'=1}^n \left( A_{j2, j'1} a_{j'}^\dagger + A_{j2, j'2} a_{j'} \right). \end{aligned} \quad (3)$$

Let  $\mathcal{H}_{\text{BdG}} = \text{span} \{a_j, a_j^\dagger\}$  denote the vector space of linear fermionic operators on  $\mathcal{F}_n$ . Let the basis of  $\mathcal{H}_{\text{BdG}}$  be denoted as  $\{|j, 1\rangle = a_j^\dagger, |j, 2\rangle = a_j\}$ ; the kets signify membership in  $\mathcal{H}_{\text{BdG}}$ . Throughout this work, small English or Greek alphabets in kets are used for vectors in  $\mathcal{H}_{\text{BdG}}$ , and capital English or Greek alphabets in kets denote states in  $\mathcal{F}_n$ .

Define an operator  $\tau_x$  that maps particles to holes and vice versa,  $\tau_x |j, 1\rangle = |j, 2\rangle$  and  $\tau_x |j, 2\rangle = |j, 1\rangle$ , i.e. that corresponds to a Pauli-X operator acting on the particle and hole blocks.  $A$  satisfies the particle-hole constraint

$$(\tau_x \mathcal{K}) A (\tau_x \mathcal{K})^{-1} = \tau_x \mathcal{K} A \mathcal{K} \tau_x = -A, \quad (4)$$

where  $\mathcal{K}$  denotes complex conjugation. Due to Eq. (4), for every eigenvalue  $\epsilon > 0$  of  $A$  there also exists an eigenvalue  $-\epsilon$ . Let  $\{\epsilon_k, k = 0, \dots, n-1\}$  denote non-negative eigenvalues of  $A$  in a non-decreasing order. Note that if zero is an eigenvalue of  $A$ , then its multiplicity  $s_0$  is even, and exactly half of these are included in the set above:  $\epsilon_k = 0$  for  $k = 0, \dots, s_0/2-1$ . Let  $\{|e_k\rangle, k = 0, \dots, n-1\}$  be an orthonormal basis of eigenvectors corresponding to eigenvalues  $\{\epsilon_k, k = 0, \dots, n-1\}$ . Then due to particle-hole constraint (4), an orthonormal basis for eigenvalues  $\{-\epsilon_k, k = 0, \dots, n-1\}$  can be chosen to be  $\{\tau_x \mathcal{K} |e_k\rangle, k = 0, \dots, n-1\}$ . With such a choice of eigenvectors,  $A$  can be expressed as

$$A = \sum_k \epsilon_k (|e_k\rangle \langle e_k| - \tau_x \mathcal{K} |e_k\rangle \langle e_k| \mathcal{K} \tau_x), \quad \epsilon_k \geq 0. \quad (5)$$

Diagonalization of the BdG operator  $A$  then casts  $\hat{A}$  into its QP form

$$\hat{A} = \sum_k \epsilon_k e_k^\dagger e_k + \text{constant}, \quad (6)$$

where  $e_k^\dagger$  and  $e_k$  are creation and annihilation operators represented by  $|e_k\rangle$  and  $\tau_x \mathcal{K} |e_k\rangle$ , respectively.

### B. Majorana zero-energy modes

With  $\hat{A}$  in Eq. (2) the Hamiltonian of the system under consideration, the  $e_k^\dagger$  and  $e_k$  are QP creation and annihilation operators, and  $\epsilon_k \geq 0$  are the QP energies. If the smallest eigenvalue  $\epsilon_0 > 0$ , then the Hamiltonian has a unique ground state  $|\Omega\rangle \in \mathcal{F}_n$  specified by the conditions  $e_k |\Omega\rangle = 0$  for all  $k$ . The state  $|\Omega\rangle$  can be interpreted as the QP vacuum, and  $e_k^\dagger |\Omega\rangle$  is a QP basis function.

Consider Kitaev's model of a one-dimensional p-wave superconductor [2], whose Hamiltonian is given by

$$\begin{aligned}\hat{H}_{\text{Kit}} = & -\mu \sum_{j=1}^n \left( a_j^\dagger a_j - \frac{1}{2} \right) \\ & + \sum_{j=1}^{n-1} \left( -w a_j^\dagger a_{j+1} + \Delta a_j a_{j+1} + \text{H.c.} \right),\end{aligned}\quad (7)$$

where  $\mu$  is the chemical potential,  $w$  is the hopping amplitude and  $\Delta$  is the superconducting pairing amplitude, and H.c. corresponds to the Hermitian conjugate. We assume for simplicity that  $\mu, w$  and  $\Delta \geq 0$  are real numbers. Diagonalizing yields

$$\hat{H}_{\text{Kit}} = \sum_{k=0}^{n-1} \epsilon_k e_k^\dagger e_k. \quad (8)$$

The parameter regime  $|\mu| < |w|$  marks the topological phase of the Kitaev Hamiltonian. For fixed parameters  $\mu, w, \Delta$  in this regime, there are two nearly degenerate ground states  $|\Omega_0\rangle$  and  $|\Omega_1\rangle$  with even and odd fermionic parity, respectively, separated by an energy  $\epsilon_0$  that is exponentially small in  $n$  [2]. In the limit of large  $n$ , the operators  $e_0, e_0^\dagger$  represent the annihilation and creation operators for the zero-energy modes. Furthermore, the global phase of  $e_0$  (and consequently of  $e_0^\dagger$ ) can be chosen such that the Majorana operators for these,

$$\gamma_1 = e_0^\dagger + e_0 \text{ and } \gamma_2 = i(e_0^\dagger - e_0), \quad (9)$$

are exponentially localized on the left and the right edges of the chain respectively, in the sense that

$$\begin{aligned}|\langle j, 1 | \gamma_1 \rangle| \approx e^{-\kappa_1 j}, \quad |\langle j, 2 | \gamma_1 \rangle| \approx e^{-\kappa_2 j}, \\ |\langle j, 1 | \gamma_2 \rangle| \approx e^{-\kappa_1(n-j)}, \quad |\langle j, 2 | \gamma_2 \rangle| \approx e^{-\kappa_2(n-j)}\end{aligned}\quad (10)$$

for some positive constants  $\kappa_1, \kappa_2$  [2, 27]. Because  $\epsilon_0 \approx 0$ , the Majorana operators commute with the system Hamiltonian up to an exponentially small correction,  $[\hat{H}_{\text{Kit}}, \gamma_1]_- \approx [\hat{H}_{\text{Kit}}, \gamma_2]_- \approx 0$ . Therefore,  $\gamma_1$  and  $\gamma_2$  are called the MZMs of  $\hat{H}_{\text{Kit}}$ . The even total-parity ground state  $|\Omega_0\rangle$  is related to the odd total-parity ground state  $|\Omega_1\rangle$  via MZMs as  $|\Omega_1\rangle \propto \gamma_1 |\Omega_0\rangle \propto \gamma_2 |\Omega_0\rangle$ . The parity operator for the zero-energy mode  $(-1)^{e_0^\dagger e_0}$  can also be expressed as  $-i\gamma_1\gamma_2$ . Therefore, the two almost degenerate ground states can be labeled by +1 and -1 eigenvalues of  $i\gamma_1\gamma_2$ . These states are also eigenstates of the total parity operator  $(-1)^{\tilde{N}}$ .

### C. Encoding a qubit in four Majorana zero-energy modes

In principle, a qubit could be stored in the two degenerate ground states of a Kitaev chain. However, the

parity superselection rule prohibits coherent superposition of the two ground states. Therefore, it is standard to use two chains for encoding one qubit, called a tetron configuration. The Hamiltonian of the tetron is defined in terms of operators

$$\{a_{p,j}, a_{p,j}^\dagger, p = 1, 2, j = 1, \dots, n\} \quad (11)$$

on the Fock space  $\mathcal{F}_{2n}$ , where  $p$  labels the two chains in the tetron, and

$$[a_{p,j}, a_{p,j'}^\dagger]_+ = \delta_{pp'} \delta_{jj'}, \quad [a_{p,j}, a_{p',j'}]_+ = 0. \quad (12)$$

By ignoring the terms connecting the two nanowires [9], and by modeling each chain by the Kitaev chain Hamiltonian, one obtains

$$\hat{H}_{\text{tet}} = \hat{H}_{1, \text{Kit}} + \hat{H}_{2, \text{Kit}}, \quad (13)$$

where  $\hat{H}_{p, \text{Kit}}$  for  $p = 1, 2$  describes the Hamiltonian of the  $p$ th chain and is obtained from Eq. (7) by replacing each  $a_j$  ( $a_j^\dagger$ ) by  $a_{p,j}$  ( $a_{p,j}^\dagger$ ), each of which act on the Fock space of the tetron  $\mathcal{F}_{2n}$ . For simplicity, assume that the parameters  $(\mu, w, \Delta)$  for the two chains in the tetron are identical, in which case the Kitaev tetron has a four-dimensional ground space when  $|\mu| < |w|$ . The logical qubit can be initialized in  $|\bar{0}\rangle, |\bar{1}\rangle$  states by preparing the system in the ground states  $|\Omega_{00}\rangle, |\Omega_{11}\rangle \in \mathcal{F}_{2n}$  respectively, both of which are +1 eigenstates of the MZM-parity operator  $(i\gamma_1\gamma_2)(i\gamma_3\gamma_4)$  [12, 13, 28–30]. Logical single-qubit Pauli gates are given by operators

$$\bar{X} \mapsto -i\gamma_1\gamma_3, \quad \bar{Y} \mapsto -i\gamma_2\gamma_3, \quad \bar{Z} \mapsto -i\gamma_1\gamma_2, \quad (14)$$

and therefore can be implemented by manipulating the MZMs.

Whereas preparing the ground states  $|\Omega_{00}\rangle, |\Omega_{11}\rangle$  amounts to initializing the qubit in the logical  $|\bar{0}\rangle, |\bar{1}\rangle$  states respectively, it would be slightly inaccurate to state that the qubit is encoded in the states  $|\Omega_{00}\rangle, |\Omega_{11}\rangle$ . Rather, the state of the qubit is completely determined by the expectation values of the Pauli observables defined in Eq.(14) together with the MZM-parity operator  $(i\gamma_1\gamma_2)(i\gamma_3\gamma_4)$ , and does not depend on whether or not the bulk (above-gap) QPs are excited. In other words, states orthogonal to the ground energy space nevertheless represent normalized logical qubit states as long as they are +1 eigenstates of the MZM parity operator. It is more accurate to state that the qubit is encoded in the even MZM-parity subspace  $\mathcal{C}_0$  of a four-dimensional tensor factor of  $\mathcal{F}_{2n}$ , on which the MZMs act non-trivially [11]. In fact, this four-dimensional space carries a representation of the algebra generated by  $\{\gamma_1, \gamma_2, \gamma_3, \gamma_4\}$ . This point is revisited in more detail in §IVB.

### D. Kitaev tetron as an error-correcting code

The ground states of the Kitaev tetron have interesting error-correcting properties [5, 17]. To describe these

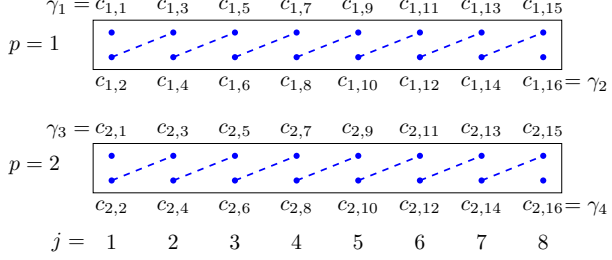


FIG. 1. Schematic of a tetron with length  $n = 8$ , comprising two Kitaev chains labeled by  $p = 1, 2$  and outlined in black rectangles. The blue dots and blue dashed lines indicate Majorana operators  $\{c_{p,j}, p = 1, 2, j = 1, \dots, n\}$  and pairing between adjacent Majorana operators at the fixed point respectively. The four MZMs hosted by the tetron are denoted by  $\{\gamma_1, \gamma_2, \gamma_3, \gamma_4\}$  (20).

properties, we first represent the Hamiltonian in Eq. (13) in terms of Majorana operators  $\{c_{p,j}, j = 1, \dots, 2n\}$ , which are defined by the relations

$$a_{p,j} = \frac{c_{p,2j-1} + ic_{p,2j}}{2}, \quad a_{p,j}^\dagger = \frac{c_{p,2j-1} - ic_{p,2j}}{2}. \quad (15)$$

The Majorana operators are self-adjoint,  $c_{p,j}^\dagger = c_{p,j}$ , and obey commutation rules

$$[c_{p,j}, c_{p',j'}]_+ = 2\delta_{p,p'}\delta_{j,j'}\mathbb{1}. \quad (16)$$

The Hamiltonian in Eq. (7) can then be expressed as

$$\hat{H}_{\text{Kit}} = \frac{i(\Delta + w)}{2} \sum_{j=1}^{n-1} c_{2j}c_{2j+1} + \frac{i(\Delta - w)}{2} \sum_{j=1}^{n-1} c_{2j-1}c_{2j+2} - \frac{i}{2} \sum_{j=1}^n \mu c_{2j-1}c_{2j}. \quad (17)$$

For the “fixed point” parameter values  $\mu = 0$  and  $w = \Delta = 1$ , one obtains

$$\hat{H}_{\text{Kit}} = \sum_{j=1}^{n-1} ic_{2j}c_{2j+1}. \quad (18)$$

The Hamiltonian for the tetron can then be expressed as

$$\hat{H}_{\text{tet}} = \sum_{p=1,2} \sum_{j=1}^{n-1} ic_{p,2j}c_{p,2j+1}. \quad (19)$$

Each chain of the Kitaev tetron hosts one MZM on each of its ends. Therefore, the tetron hosts four MZMs in total, labeled by

$$\gamma_1 = c_{1,1}, \quad \gamma_2 = c_{1,2n}, \quad \gamma_3 = c_{2,1}, \quad \gamma_4 = c_{2,2n} \quad (20)$$

in Fig. 1.

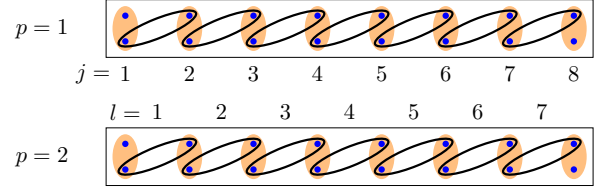


FIG. 2. Schematic of stabilizers and elementary errors for a tetron of length  $n = 8$ . The support of each stabilizer  $Q_{p,l}$  is outlined in black, and the support of each elementary error  $E_{p,j}$  is shaded in orange.

The even-parity ground states of the Kitaev tetron are known to form a Majorana fermionic stabilizer code  $\mathcal{C}_{\text{GS}}$ , which can in principle correct local parity preserving errors [5, 17, 31]. The explicit dependence of  $\mathcal{C}_{\text{GS}}$  on the length  $n$  of the Kitaev tetron is omitted for brevity. The four-dimensional ground space of the Kitaev tetron is the subspace defined by the stabilizer generators (see Fig. 2)

$$\{Q_{p,l} = -ic_{p,2l}c_{p,2l+1}, \quad p = 1, 2, l = 1, \dots, n-1\}, \quad (21)$$

and the two even MZM-parity ground states are stabilized by the MZM-parity operator

$$Q_{\text{parity}} = (-i\gamma_1\gamma_2)(-i\gamma_3\gamma_4) = -\gamma_1\gamma_2\gamma_3\gamma_4. \quad (22)$$

In fact, the Hamiltonian of the tetron can be expressed in terms of the stabilizers as

$$\hat{H}_{\text{tet}} = - \sum_{p=1,2} \sum_{l=1}^{n-1} Q_{p,l}. \quad (23)$$

Measurement of these stabilizers leads to discretization of even-parity noise processes, and the resulting discretized processes are products of elementary errors

$$\{E_{p,j} = ic_{p,2j-1}c_{p,2j}, \quad p = 1, 2, j = 1, \dots, n\}. \quad (24)$$

Any arbitrary even-parity error  $E$  can be expressed as a linear combination of terms that are products of elementary errors and stabilizers in Eq. (21), that is

$$E = \sum_r E_r, \quad E_r = \prod_{p=1,2} \prod_{j \in \mathcal{J}_{r,p}} E_{p,j} \prod_{l \in \mathcal{L}_{r,p}} Q_{p,l}, \quad (25)$$

where  $\mathcal{J}_{r,p} \subset \{1, \dots, n\}$  and  $\mathcal{L}_{r,p} \in \{1, \dots, n-1\}$ . The weight of  $E$ , denoted by  $\text{wt}(E)$ , is two times the maximum number of elementary errors on a single chain present in the decomposition of any one of the terms in the linear combination, that is

$$\text{wt}(E) = 2 \max_{r,p} |\mathcal{J}_{r,p}|. \quad (26)$$

The code  $\mathcal{C}_{\text{GS}}$  can correct exactly any even-parity error  $E$  with  $\text{wt}(E) \leq n - 1$ .

### E. Covariance matrix framework

In this section, we recall some basic definitions and propositions in the covariance matrix formalism for fermionic Gaussian states [32]. These propositions are used for simulating qubits encoded in certain error-detecting codes on a tetron.

**Definition II.1.** The covariance matrix of a  $|\Psi\rangle \in \mathcal{F}_{2n}$  is the antisymmetric matrix with entries

$$M_{p,j;p',j'} = -\frac{i}{2} \langle \Psi | [c_{p,j}, c_{p',j'}]_- | \Psi \rangle, \quad p, p' \in \{1, 2\}, \quad j, j' \in \{1, \dots, 2n\}. \quad (27)$$

Note that in Eq. (27),  $(p, j)$  and  $(p', j')$  denote the row and column indices of  $M$ , respectively.

**Lemma II.2.** For  $\mu = 0$  and  $w = \Delta = 1$ , the covariance matrix  $M_\zeta$  of the ground state of  $\hat{H}_{\text{tet}}$  satisfying  $\langle \Psi | (-ic_{p,1}c_{p,2n}) | \Psi \rangle = (-1)^\zeta$  with  $\zeta \in \{0, 1\}$ , has only non-zero entries

$$[M_\zeta]_{p,2j;p,2j+1} = 1, \quad [M_\zeta]_{p,1;p,2n} = (-1)^\zeta, \quad p = 1, 2, \quad j = 1, \dots, n-1. \quad (28)$$

The next lemma makes use of the Majorana operator basis  $\{|c_{p,j}/\sqrt{2}\rangle, p = 1, 2, j = 1, \dots, 2n\}$  of  $\mathcal{H}_{\text{BdG}}$ , where

$$\begin{aligned} \left| \frac{c_{p,2j-1}}{\sqrt{2}} \right\rangle &= \frac{|p, j, 1\rangle + |p, j, 2\rangle}{\sqrt{2}}, \\ \left| \frac{c_{p,2j}}{\sqrt{2}} \right\rangle &= -i \frac{|p, j, 1\rangle - |p, j, 2\rangle}{\sqrt{2}}. \end{aligned} \quad (29)$$

**Lemma II.3.** Let  $\hat{H}$  be a Hamiltonian quadratic in Majorana operators  $\{c_{p,j}\}$ , and let  $H$  be the corresponding BdG Hamiltonian expressed in the Majorana operator basis. If  $M$  is the covariance matrix of  $|\Psi\rangle$ , then the covariance matrix of  $e^{-i\hat{H}t} |\Psi\rangle$  is  $RMR^T$  with  $R = e^{iHt}$ .

**Lemma II.4.** Consider an ordered list of operators  $L_1, \dots, L_{2m}$  such that every operator  $L_j$  is a linear combination of the Majorana operators  $c_{p,1}, \dots, c_{p,2n}$  with complex coefficients. For  $|\Psi\rangle \in \mathcal{F}_{2n}$ , define an anti-symmetric  $2m \times 2m$  complex matrix  $A$  such that  $A_{jj'} = \langle \Psi | L_j L_{j'} | \Psi \rangle$  for  $j < j'$ . Then

$$\langle \Psi | L_1 \dots L_{2m} | \Psi \rangle = \text{Pf}(A), \quad (30)$$

where  $\text{Pf}(\bullet)$  denotes the Pfaffian.

### III. MODEL OF QUASIPARTICLE DETECTION

We now construct a model for QP detection with finite spatial resolution. Finite spatial resolution is important for two reasons. First, such a model could be easier to realize in some systems. Second, a detector with high spatial resolution is potentially more advantageous for detecting local errors, as is discussed later.

### A. Quasiparticle position operator

A local measurement of QPs is conceivable if the measurement probe can couple to the position of the QPs. Therefore, to model a detector with finite spatial resolution, one must first derive an analog of the position operator for QP excitations. Define the position operator for fermions on one of the chains as  $\hat{X} = \sum_j j a_j^\dagger a_j$  (this is the position analog of the current operator). First,  $\hat{X}$  is a quadratic operator, which means that it acts independently on the particles. Second,  $\hat{X}$  commutes with the number operator  $\hat{N} = \sum_j a_j^\dagger a_j$ , which means that a projective measurement of  $\hat{X}$  on a Fock state with a fixed number of particles does not alter the number of particles. In other words,  $\hat{X}$  is a nondemolition measurement [33]. Third, the BdG representation of  $\hat{X}$ , which is  $X = \sum_j j(|j, 1\rangle \langle j, 1| - |j, 2\rangle \langle j, 2|)$ , satisfies  $\langle \psi | X | \psi \rangle = \sum_j j |\psi_j|^2$  for any creation operator  $|\psi\rangle = \sum_j \psi_j |j, 1\rangle \in \mathcal{H}_{\text{BdG}}$ , and similarly satisfies  $(\langle \psi | \tau_x \mathcal{K} X (\tau_x \mathcal{K} | \psi \rangle) = -\sum_j j |\psi_j|^2$  for the corresponding annihilation operator.

Taking inspiration from the defining properties of  $\hat{X}$ , the QP position operator  $\hat{X}_{\text{qp}}$  should satisfy the following desiderata:

1.  $\hat{X}_{\text{qp}}$  acts independently on QPs.
2. A projective measurement of  $\hat{X}_{\text{qp}}$  is a non-demolition measurement in the sense that for any eigenstate of  $\hat{N}_{\text{qp}}$ , the post-measurement state is also an eigenstate of  $\hat{N}_{\text{qp}}$  with the same eigenvalue.
3. If a QP is localized near site  $j$ , then  $\langle \psi | X_{\text{qp}} | \psi \rangle \approx j$ .

For the first property to be satisfied,  $\hat{X}_{\text{qp}}$  must be quadratic in QP creation and annihilation operators  $\{e_k^\dagger, e_k, k = 1, \dots, n-1\}$ . While MZMs described by operators  $e_0^\dagger, e_0$  are also technically QPs, they are excluded from the set of QPs as they are not responsible for leakage from the ground-state manifold. For the second property to be satisfied,  $\hat{X}_{\text{qp}}$  must commute with the QP number operator  $\hat{N}_{\text{qp}}$ .

To construct the operator  $\hat{X}_{\text{qp}}$ , consider its action on the BdG space. In the following,  $H$  is a Hermitian operator on  $\mathcal{H}_{\text{BdG}}$  satisfying the particle-hole constraint in Eq. (4). Let  $\{|e_k\rangle, k = 0, 1, \dots, n-1\}$  be the eigenvectors of  $H$  with non-negative eigenvalues  $\{\epsilon_k, k = 0, 1, \dots, n-1\}$  as above. Let

$$P_{\text{qp}} = \sum_{k=1}^{n-1} |e_k\rangle \langle e_k| \quad (31)$$

be the projector on the space of QP creation operators, and

$$P_{\overline{\text{qp}}} = (\tau_x \mathcal{K}) P_{\text{qp}} (\mathcal{K} \tau_x) = \sum_{k=1}^{n-1} (\tau_x \mathcal{K}) |e_k\rangle \langle e_k| (\mathcal{K} \tau_x) \quad (32)$$

be the projector on the space of QP annihilation operators. Define  $\tilde{X} = NX = \sum_j j(|j,1\rangle\langle j,1| + |j,2\rangle\langle j,2|)$ .

**Theorem III.1.** *Let  $P_{\text{qp}}, \hat{N}_{\text{qp}}$  and  $\tilde{X}$  be as defined above.*

1. *The BdG operator defined by*

$$X_{\text{qp}} = P_{\text{qp}}\tilde{X}P_{\text{qp}} - P_{\overline{\text{qp}}}\tilde{X}P_{\overline{\text{qp}}}, \quad (33)$$

*satisfies the particle-hole constraint, Eq. (4).*

2. *The observables  $\hat{X}_{\text{qp}}$  and  $\hat{N}_{\text{qp}}$  can be observed simultaneously, i.e.,*

$$[\hat{X}_{\text{qp}}, \hat{N}_{\text{qp}}]_- = 0. \quad (34)$$

3. *For all  $|\psi\rangle \in \text{span}\{|e_k\rangle, k = 1, \dots, n-1\}$ ,*

$$\begin{aligned} \langle\psi|X_{\text{qp}}|\psi\rangle &= -\langle\psi|(\tau_x\mathcal{K})X_{\text{qp}}(\mathcal{K}\tau_x)|\psi\rangle \\ &= \sum_j j(|\langle j,1|\psi\rangle|^2 + |\langle j,2|\psi\rangle|^2). \end{aligned} \quad (35)$$

*Proof.* The particle-hole constraint follows from the fact that  $(\tau_x\mathcal{K})P_{\text{qp}}(\mathcal{K}\tau_x) = P_{\overline{\text{qp}}}$  and  $(\tau_x\mathcal{K})\tilde{X}(\mathcal{K}\tau_x) = \tilde{X}$ . The second statement, namely  $[\hat{X}_{\text{qp}}, \hat{N}_{\text{qp}}]_- = 0$ , follows from the relations  $N_{\text{qp}} = P_{\text{qp}} - P_{\overline{\text{qp}}}$ ,  $P_{\text{qp}}^2 = P_{\text{qp}}$ ,  $P_{\overline{\text{qp}}}^2 = P_{\overline{\text{qp}}}$  and  $P_{\text{qp}}P_{\overline{\text{qp}}} = 0$ , where  $N_{\text{qp}}$  is the BdG representation of  $\hat{N}_{\text{qp}}$ . For the third statement, using  $P_{\text{qp}}|\psi\rangle = |\psi\rangle$  and  $P_{\overline{\text{qp}}}|\psi\rangle = 0$ , one obtains  $\langle\psi|P_{\text{qp}}\tilde{X}P_{\text{qp}}|\psi\rangle = \langle\psi|\tilde{X}|\psi\rangle$ . A straightforward calculation yields

$$\begin{aligned} \langle\psi|\tilde{X}|\psi\rangle &= \langle\psi|\tilde{X}\sum_{j=1}^N (\langle j,1|\psi\rangle|j,1\rangle + \langle j,2|\psi\rangle|j,2\rangle) \\ &= \langle\psi|\sum_{j=1}^N (j\langle j,1|\psi\rangle|j,1\rangle + j\langle j,2|\psi\rangle|j,2\rangle) \\ &= \sum_j j(|\langle j,1|\psi\rangle|^2 + |\langle j,2|\psi\rangle|^2). \end{aligned} \quad (36)$$

□

## B. Exponential localization of Wannier quasiparticles

Next we show that the eigenmodes of  $\hat{X}_{\text{qp}}$  (represented by eigenvectors of  $X_{\text{qp}}$ ) are exponentially localized in space. These localized eigenmodes are the analogs of exactly localized position eigenmodes  $\{a_j^\dagger, a_j\}$  for the fermionic particles. This localization property plays an important role in making the QP detection measurements very powerful for the purpose of suppressing logical errors.

Suppose  $X_{\text{qp}}$  has the spectral decomposition

$$X_{\text{qp}} = \sum_{l=1}^{n-1} x_l [|\phi_l\rangle\langle\phi_l| - (\tau_x\mathcal{K})|\phi_l\rangle\langle\phi_l|(\mathcal{K}\tau_x)], \quad (37)$$

with  $x_l \geq x_{l'}$  if  $l > l'$  and  $x_l > 0$  for all  $l$ . Then

$$\hat{X}_{\text{qp}} = \sum_{l=1}^{n-1} x_l \phi_l^\dagger \phi_l, \quad (38)$$

where  $\phi_l^\dagger$  is the operator represented by  $|\phi_l\rangle$ . Given that  $\sum_{l=1}^{n-1} |\phi_l\rangle\langle\phi_l| = \sum_{k=1}^{n-1} |e_k\rangle\langle e_k| = P_{\text{qp}}$ , then

$$\sum_{l=1}^{n-1} \phi_l^\dagger \phi_l = \sum_{k=1}^{n-1} e_k^\dagger e_k = \hat{N}_{\text{qp}}. \quad (39)$$

The states  $\{|\phi_l\rangle\}$  represent Wannier QP (WQP henceforth) excitations of the system. Therefore,  $\phi_l$  and  $\phi_l^\dagger$  describe the annihilation and creation of the  $l$ th WQP. Note that the index  $l$  above ranges from 1 to  $n-1$ , and not to  $n$ , as the MZMs are deliberately excluded from the set of QPs while constructing  $\hat{X}_{\text{qp}}$ . The same index  $l$  is used to enumerate the WQPs and the stabilizers in Eq. (21); indeed, WQPs and stabilizers are closely related, as discussed in §IV A.

While it is mathematically convenient to prove that the Wannier functions are exponentially localized by making use of an infinite system, this work is expressly focused on systems with boundary terminations. We therefore prove our results for long but finite Kitaev chains, for Hamiltonians that model a topological superconductor with weak disorder and that host only one MZM on each edge. Let  $\{|j, m\rangle : j \in \mathbb{Z}^+, m \in \{1, \dots, D\}\}$  denote the standard basis of  $\ell^2(\mathbb{Z}^+ \times \mathbb{C}^D) = \mathcal{H}_{\text{BdG}}$ . Next, let  $H$  be a Hermitian operator on  $\mathcal{H}_{\text{BdG}}$  and suppose that  $H$  has exponentially decaying hopping and pairing correlations in the sense that for some constants  $(C, \kappa)$ ,

$$|\langle j, m|H|j', m'\rangle| \leq Ce^{-\kappa|j-j'|}. \quad (40)$$

Such an operator is said to be exponentially localized (see Def. A.1 for a rigorous definition.) Suppose that there exists a lower bound  $\delta > 0$  on the energy gap, i.e.,  $\sigma(H) \cap (0, \delta) = \emptyset$  where  $\sigma(\bullet)$  denotes the spectrum of its argument. This condition is equivalent to requiring a bulk energy gap at least  $\delta$  and no localized energy modes other than MZMs with energy smaller than  $\delta$ .

**Lemma III.2.** *There exist constants  $(C', \kappa')$  so that*

$$|\langle j, m|P_{\text{qp}}|j', m'\rangle| \leq C'e^{-\kappa'|j-j'|}. \quad (41)$$

In other words,  $P_{\text{qp}}$  is exponentially localized.

**Theorem III.3.** *Suppose  $P_{\text{qp}}$  is an exponentially localized operator on  $\ell^2(\mathbb{Z}^+ \times \mathbb{C}^D)$ . Then*

1. *The operator  $X_{\text{qp}}$  has purely discrete spectrum on range( $P_{\text{qp}}$ )).*
2. *There exist constants  $(C_{\text{qp}}, \kappa_{\text{qp}})$  depending only of  $P_{\text{qp}}$ , such that if  $|\phi\rangle \in \text{range}(P_{\text{qp}})$  satisfies the eigenvalue equation*

$$X_{\text{qp}}|\phi\rangle = x|\phi\rangle \quad (42)$$

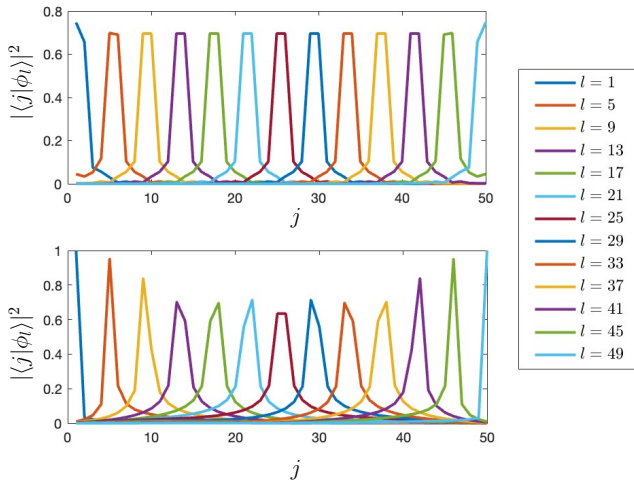


FIG. 3. The amplitude of a few WQP excitations for parameters  $\mu = 0.3, w = 1, \Delta = 0.4$  (top panel) and  $\mu = 0.99, w = 1, \Delta = 0.05$  (bottom panel). The tetron length is  $n = 50$  in both the plots.

for some  $x > 0$ , then  $|\phi\rangle$  is exponentially localized about the point  $x$  in the sense that

$$|\langle j, m | \phi \rangle| \leq C_{\text{qp}} e^{-\kappa_{\text{qp}} |j-x|} \quad (43)$$

The proofs of Lemma III.2 and Theorem III.3 are provided in the Appendices B and C respectively, and they utilize some preliminary results about exponentially localized operators proved in Appendix A.

Computing WQP operators numerically only requires the diagonalization of the operator  $X_{\text{qp}}$ . The amplitude of some WQP operators are plotted in Fig. 3. Observe that the WQPs are tightly localized for parameters away from the topological phase boundary, Fig. 3 (top panel). The spatial extent increases as one approaches the topological phase boundary, Fig. 3 (bottom panel), reflecting the closure of the many body gap.

### C. From Wannier quasiparticles to projective measurements

A QP detector with inverse resolution  $\lambda \in \mathbb{Z}^+$  is characterized by the set of projective measurements that it can perform. For  $l_{\min}, l_{\max} \in \{1, \dots, n-1\}$  with  $l_{\min} \leq l_{\max}$ , one can define the discrete interval

$$[[l_{\min}, l_{\max}]]_p = \{(p, l_{\min}), (p, l_{\min}+1), \dots, (p, l_{\max})\} \quad (44)$$

on the  $p$ th chain. Consequently,  $[[l_{\min}, l_{\max}]]_p \subseteq [[1, n-1]]_p$  for any valid  $[[l_{\min}, l_{\max}]]_p$ . Let

$$|[[l_{\min}, l_{\max}]]_p| = l_{\max} - l_{\min} + 1 \quad (45)$$

be the length of the interval  $[[l_{\min}, l_{\max}]]_p$ . For any such  $I_p = [[l_{\min}, l_{\max}]]_p$  on the  $p$ th chain, the operator

$$\hat{N}_{\text{qp}}^{I_p} = \sum_{(p,l) \in I_p} \phi_{p,l}^\dagger \phi_{p,l}, \quad (46)$$

counts the number of QPs in the interval  $I_p$ . Evidently,  $\hat{N}_{\text{qp}}^{[[1, n-1]]_p} = \sum_{k=1}^{n-1} e_k^\dagger e_k$ . Note  $l_{\max} \leq n-1$  because we exclude the MZMs from the QPs, and therefore we have only  $n-1$  WQPs.

We now define an ‘on-off’ detector measurement for QPs in an interval  $I_p$ . Such a measurement yields 0 if no QPs are detected in the interval  $I_p$ , and yields 1 if at least one QP is detected. Such a measurement is analogous to number non-resolving photon measurement commonly used in quantum optics [33]. Let us first introduce the heaviside function on positive integers

$$\theta(j) = \begin{cases} 0 & \text{if } j = 0 \\ 1 & \text{if } j > 0 \end{cases}. \quad (47)$$

Then

$$\theta(\hat{N}_{\text{qp}}^{I_p}) = \mathbb{1} - \prod_{(p,l) \in I_p} \phi_{p,l} \phi_{p,l}^\dagger \quad (48)$$

is an orthogonal projector on the Fock states in which at least one QP is excited in the interval  $I$ ; this can be verified by observing that the second term on the right-hand side annihilates any such state. For the interval  $I_p$ , we associate the projective measurement

$$\mathcal{M}_{I_p} = \{\theta(\hat{N}_{\text{qp}}^{I_p}), \mathbb{1} - \theta(\hat{N}_{\text{qp}}^{I_p})\}, \quad (49)$$

which models a number non-resolving detection of the QPs in the interval  $I_p$ . The measurement  $\mathcal{M}_{I_p}$  can be performed by a detector with inverse resolution  $\lambda$  if  $|I_p| \geq \lambda$ . Such a detector can also perform simultaneous measurements  $\{\mathcal{M}_{I_{p,j}}\}$  as long as the intervals  $\{I_{p,j}\}$  are individually longer than  $\lambda$  and are pairwise disjoint, that is  $I_{p,j} \cap I_{p,j'} = \delta_{jj'} I_{p,j}$ . Any interval on the  $p=1$  chain is by definition disjoint with respect to any interval on the  $p=2$  chain.

In summary, in quadratic fermionic systems such as the Kitaev tetron, the QP excitations are eigenmodes of the many-body Hamiltonian. A position-resolving detector is a device that approximately measures the position of a QP without destroying or creating any QPs. The eigenmodes of this operator are Wannier QPs, which are proven to be exponentially localized. A detector then determines if any Wannier QPs are excited in a given interval of length, which is bounded from below by the finite spatial resolution.

This model of QP detection is used throughout to describe erasure conversion in Majorana qubits and for assessing its performance. Note that an experimental probe that couples to the QP position operator can perform the QP detection measurements described above. In general, any detector that is sufficiently local and that detects the QPs only above the energy gap, i.e., excluding

MZMs, will achieve the required measurements. Unfortunately, the latter requirement is not met by transport measurements, and therefore warrants further investigation. Note also that the exponential localization of WQPs holds for generic models of one-dimensional topological superconductors. Therefore, our results extend naturally to the corresponding models of Majorana tetron qubits.

#### IV. ERASURE CONVERSION BY QUASIPARTICLE DETECTION

We consider next the incorporation of general QP detection measurements in the error-correction framework. This is achieved by a process known as ‘erasure conversion’, in which additional capabilities at the hardware level are used to detect a set of errors that may have occurred on each qubit. Upon resetting or erasing the qubits on which errors are detected, these errors turn into erasure errors [18–21]. The main strength of erasure conversion is that it can be made compatible with a concatenation of any outer quantum error-correcting code with a suitable choice of decoder. The analysis is based on the observation that erasure conversion is equivalent to implementing an error-detecting code at the hardware level. In the following, we first relate QP detection to certain collective stabilizer measurements and then construct error-detecting stabilizer codes that describe erasure conversion.

##### A. From quasiparticle detection to stabilizer measurements

We begin the construction of the required error-detecting codes by first making a connection between the quasiparticle detectors and the stabilizers of the Kitaev tetron code at the fixed point. The WQP operators  $\{\phi_{p,l}\}$  at the fixed point ( $\mu = 0, w = \Delta = 1$ ) are straightforward to calculate, and are given by

$$\phi_{p,l} = (c_{p,2l} - ic_{p,2l+1})/2, \quad l = 1, \dots, n-1, \quad (50)$$

with the corresponding eigenvalues being

$$x_{p,l} = l + 1/2. \quad (51)$$

Therefore

$$(-1)^{\phi_{p,l}^\dagger \phi_{p,l}} = (-1)^{\hat{N}_{\text{qp}}^{[[l,l]]_p}} = Q_{p,l}, \quad l = 1, \dots, n-1, \quad (52)$$

where  $[[l,l]]_p = \{(p,l)\}$  is a discrete interval of unit length on the  $p$ th chain. Thus, each of the stabilizers in Eq. (21) is in fact the parity operator for the corresponding WQP

degree of freedom, at the fixed point. The effect of each of the errors in Eq. (24) is to excite or de-excite either one (for  $l \in \{1, n-1\}$ ) or two (for  $l \in \{2, \dots, n-1\}$ ) WQPs.

##### B. Quasiparticle detection-based error-detecting codes

In this section, we describe error-detecting codes that are implementable with a QP detector of a certain spatial resolution. We then define and construct some simple Majorana fermionic error-detecting codes with gauge degrees of freedom. The motivation for this is quite different from other subsystem codes in the literature, including the gauge color code [34]. In the latter, gauge degrees of freedom are fully accessible and are meant to facilitate the implementation of a universal transversal gate set. In contrast, the gauge degrees of freedom in this work are completely inaccessible; one could describe the codes purely as stabilizer subspace codes by eliminating all gauge degrees of freedom from the description, but the gauge degrees are retained in this work as they permit a direct connection with the underlying tetron Fock space  $\mathcal{F}_{2n}$ .

In the absence of QP detection, the qubit is encoded in the space  $\mathcal{C}_0$  in a tetron, as explained in §II C. This can be interpreted as an error-detecting stabilizer code of four MZMs, with the MZM-parity operator  $(i\gamma_1\gamma_2)(i\gamma_3\gamma_4)$  the only stabilizer. This code can detect any odd MZM-parity error. In this sense, the remaining  $4n - 4$  Majorana fermionic operators, which correspond to the bulk QP excitations on the two chains, are treated as gauge degrees of freedom [35, 36]. Consequently, any process supported on the bulk QPs does not affect the state of the encoded qubit. Treating bulk QPs as gauge degrees of freedom is beneficial if detection of QPs is inaccessible, because the detection of odd MZM-parity errors alone is possible without requiring the detection of QPs. In contrast, the encoding in  $\mathcal{C}_{\text{GS}}$  discussed in §IID treats all bulk QPs as stabilizers; indeed, following the discussion in §IV A, the stabilizers measure the occupation parity of each bulk QP mode. Thus, in this picture there are no gauge degrees of freedom, and the encoding discussed in §IID could be implemented if some sort of QP detection were accessible. Furthermore, this could be highly beneficial, as individual stabilizer measurements can detect any even total-parity error of weight  $\leq 2n - 2$ .

We begin by exploring the subsystem decompositions associated with the codes discussed in §II C and §IID. A modified Jordan-Wigner transformation  $\nu$  can be used to map the Hilbert space of  $2n$  qubits onto  $\mathcal{F}_{2n}$ . For reasons that will soon be obvious, label the first two qubits ‘MZM’ and ‘parity’, and the remaining  $2n - 2$  qubits by tuples  $\{(p,l), p = 1, 2, l = 1, \dots, n-1\}$ . The invertible mapping is given by (see Fig. 4)

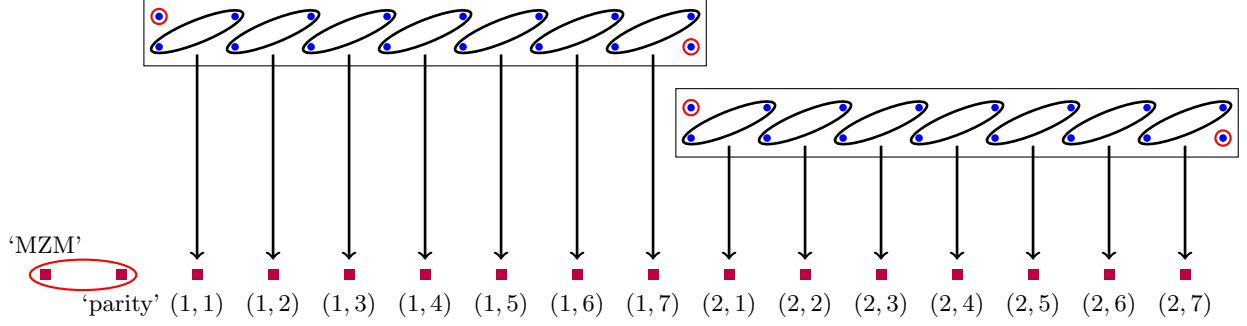


FIG. 4. Schematic of the mapping from Majorana operators (blue dots) to qubits (brown squares) for a tetron of length  $n = 8$ . The arrows show the mapping of  $Q_{p,l}$  to  $Z_{p,l}$ . The MZMs (circles in red) map to operators on the ‘MZM’ and the ‘parity’ qubits outlined in red.

$$\begin{aligned}
 Z_{\text{MZM}} &\xrightarrow{\nu} i\gamma_1\gamma_2, & X_{\text{MZM}} &\xrightarrow{\nu} i\gamma_2\gamma_3, & Z_{\text{parity}} &\xrightarrow{\nu} -\gamma_1\gamma_2\gamma_3\gamma_4, & X_{\text{parity}} &\xrightarrow{\nu} \gamma_4, \\
 Z_{p,l} &\xrightarrow{\nu} Q_{p,l}, & X_{p,l} &\xrightarrow{\nu} (-\gamma_1\gamma_2\gamma_3\gamma_4)(\prod_{l=1}^{n-1} Q_{1,l})^{\delta_{p,2}}(\prod_{l'=1}^{l-1} Q_{p,l'})(\phi_{p,2l}^\dagger + \phi_{p,2l}), & p &= 1, 2, & l &= 1, \dots, n-1. \quad (53)
 \end{aligned}$$

Similar to the standard Jordan-Wigner transformation, Eq. (53) maps some local fermionic operators to non-local qubit operators. Consequently, local fermionic errors in Eq. (24) are mapped to non-local qubit errors. The fact that  $X_1$  and  $Z_1$  are highly non-local fermionic operators is key to understanding the utility of these codes.

It is straightforward to verify that the MZMs act non-trivially only on the ‘MZM’ and ‘parity’ qubits, and act trivially on the remaining  $2n - 2$  qubits. These  $2n - 2$  qubits indeed serve as the gauge degrees of freedom in the code  $\mathcal{C}_0$  discussed in §II C. All Pauli operators supported on the gauge qubits alone belong to the gauge group. The only stabilizer of  $\mathcal{C}_0$ , which is the MZM-parity operator  $(i\gamma_1\gamma_2)(i\gamma_3\gamma_4)$ , corresponds to  $Z_{\text{parity}}$  under the map  $\nu$ . In other words, the projector on the stabilizer space projects onto the  $|0\rangle_{\text{parity}}$  state of the ‘parity’ qubit. When the ‘parity’ qubit is in the  $|0\rangle_{\text{parity}}$  state, the state of the ‘MZM’ qubit is the logical state of  $\mathcal{C}_0$ . That is,  $|\bar{\zeta}\rangle = |\zeta\rangle_{\text{MZM}}|0\rangle_{\text{parity}}|\psi\rangle_{\{(p,l)\}}$  for  $\zeta = 0, 1$ , where  $|\psi\rangle$  is an arbitrary state of the gauge qubits.

In contrast, for the code  $\mathcal{C}_{\text{GS}}$  discussed in §II D, the logical states are  $|\bar{\zeta}\rangle = |\zeta\rangle_{\text{MZM}}|0\rangle_{\text{parity}} \otimes_{(p,l)} |0\rangle_{(p,l)}$ . These states in fact span the stabilizer space, and there are no gauge qubits. Observe that in both the codes  $\mathcal{C}_0$  and  $\mathcal{C}_{\text{GS}}$ , the logical qubit is encoded in the subsystem invariant under  $\mathcal{G}$  of the subspace stabilized by  $\mathcal{S}$ . This in fact follows directly from the definition of subsystem codes [35].

Consider an error-detecting code  $\mathcal{C}$  in which a subset

$$S \subseteq \{\text{‘parity’}, (p, l), p = 1, 2, l = 1, \dots, n-1\} \quad (54)$$

of qubits act as stabilizer qubits and the complementary subset of qubits

$$G = \{\text{‘parity’}, (p, l), p = 1, 2, l = 1, \dots, n-1\} \setminus S \quad (55)$$

act as the gauge qubits. Thus, the codes we consider encode one logical qubit, the state of which is identical to the state of the ‘MZM’ qubit when the stabilizer qubits labeled by  $\{r \in S\}$  are all in  $|0\rangle_r$  state. If any of the stabilizer qubits is in  $|1\rangle_r$  state, then the state is outside the code space. The stabilizer group for such a code is

$$\mathcal{S} = \langle\{Z_r, r \in S\}\rangle, \quad (56)$$

where  $\langle\{\bullet\}\rangle$  denotes the group generated by  $\{\bullet\}$ . The gauge group  $\mathcal{G}$  is generated by all Pauli operators acting on the qubits in  $G$  [36] together with the stabilizers, that is

$$\mathcal{G} = \langle\{Z_r, r \in S\} \cup \{i\} \cup \{X_r, Z_r, r \in G\}\rangle. \quad (57)$$

In fact, as is well known in general,  $\mathcal{G}$  alone uniquely defines the code  $\mathcal{C}$ . For this code,  $l_{\text{even}}(\mathcal{C})$  is defined to be the length of the smallest weight Majorana fermionic operator which implements a non-trivial logical operation. Any error of weight less than  $l_{\text{even}}$  is detectable given access to measurements of all stabilizers in Eq. (21) individually.

In this sense, the set  $S$  of stabilizer qubits uniquely defines an error-detecting code. For a positive integer  $d < n/2$ , the code  $\mathcal{C}_d$  consists of the stabilizer qubits

$$\begin{aligned}
 \mathcal{S}_d = & \text{‘parity’} \cup \{(p, l), p = 1, 2, l = 1, \dots, d\} \\
 & \cup \{(p, l), p = 1, 2, l = n-d, \dots, n-1\}. \quad (58)
 \end{aligned}$$

We denote the corresponding stabilizer group by  $\mathcal{S}_d$  and the corresponding gauge group by  $\mathcal{G}_d$ . Therefore,  $\mathcal{C}_d$  is the code uniquely defined by its gauge group  $\mathcal{G}_d$ .

The image of the gauge group  $\mathcal{G}_d$  under the mapping  $\nu$  in Eq. (53), namely  $\nu(\mathcal{G}_d)$ , yields a Majorana fermionic code  $\nu(\mathcal{C}_d)$ . For brevity, we drop  $\nu$  from the notation

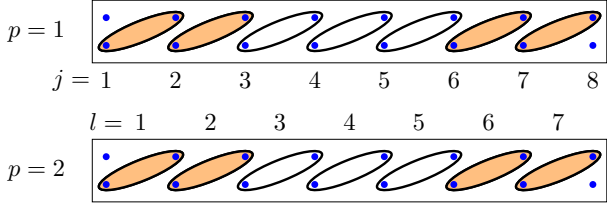


FIG. 5. The support of stabilizers (shaded) of  $\mathcal{C}_2$  on a tetron of length  $n = 8$ .

henceforth; whether an operator is in the qubit Hilbert space or the tetron Fock space will be clear from the context. The following lemma provides the even-parity distance  $l_{\text{even}}(\mathcal{C}_d)$ .

**Lemma IV.1.** *The even-parity distance of  $\mathcal{C}_d$  is*

$$l_{\text{even}}(\mathcal{C}_d) = 4d + 4. \quad (59)$$

*Proof.* The proof is obvious given the locations of the stabilizers on the Kitaev tetron (see Fig. 5). Any operator that implements a logical operator must contain terms quadratic in MZMs. An operator with even total-parity that commutes with all stabilizers and includes two MZMs must have weight  $\geq 4d + 4$ .  $\square$

### C. Error detectability with respect to quasiparticle detection

The discussion of error-correcting and error-detecting codes in the literature assumes that noisy measurements and unitary operations on all physical degrees of freedom are accessible. Since the resources available for stabilizer measurements in the system under consideration are physically constrained, it is important to clarify which error-detecting codes are compatible with these constraints. QP detection with spatial resolution  $\lambda \leq 1$  allows measurement of individual stabilizers, which enables the detection of any error with weight less than  $l_{\text{even}}$ . This is not the case if only QP detections with low spatial resolutions are accessible, however. It is important, therefore, to identify which codes remain detectable for a given  $\lambda$ , as all errors with weight less than  $l_{\text{even}}$  can be detected by a QP detector with spatial resolution  $\lambda$ .

**Definition IV.2.** The code  $\mathcal{C}_d$  is error-detecting with respect to  $\lambda$  if there exists a set of disjoint intervals  $\mathcal{I} = \{I_{p,j} \subseteq \{1, \dots, n\}_p, |I_{p,j}| \geq \lambda\}$  such that

$$P_{\text{parity}} P_{\mathcal{I}} = P_{\mathcal{S}}, \quad (60)$$

where

$$P_{\mathcal{I}} = \prod_{p,j} (\mathbb{1} - \theta(\hat{N}_{\text{qp}}^{I_{p,j}})) \quad (61)$$

is the projector on the space with no detectable QP excitations,

$$P_{\mathcal{S}} = \prod_{r \in S_d} \left( \frac{\mathbb{1} + Q_r}{2} \right) \quad (62)$$

is the projector on the stabilizer space, and

$$P_{\text{parity}} = \frac{(\mathbb{1} + Q_{\text{parity}})}{2} \quad (63)$$

is the projector on the even MZM-parity space.

This definition implies that any error that takes the system out of the stabilizer space is detectable. More concretely, for any even total-parity error  $E$  with  $\text{wt}(E) < 4d + 4$ ,

$$\text{tr}_G(P_{\text{parity}} P_{\mathcal{I}} E P_{\mathcal{S}} E^\dagger P_{\mathcal{I}} P_{\text{parity}}) \propto \text{tr}_G(P_{\mathcal{S}}). \quad (64)$$

In other words, if the outcomes of all binary measurements  $\{\mathcal{M}_{I_{p,j}}\}$  are 0, then the post-measurement state is equal to the code state before being subjected to the error operator  $E$ . Consequently, if an even total-parity error  $E$  is not detectable and acts non-trivially on the logical qubit, then  $\text{wt}(E) \geq 4d + 4$ .

**Theorem IV.3.** *For any  $d < n/2$ , the code  $\mathcal{C}_d$  is error-detecting with respect to  $\lambda$  for  $\lambda \leq d$ .*

*Proof.* It suffices to show that  $P_{\mathcal{I}}$  defined in Eq. (61) with respect to the intervals

$$I_{p,1} = \{1, \dots, d\}_p, \quad I_{p,2} = \{n - d, \dots, n - 1\}_p, \quad p = 1, 2 \quad (65)$$

satisfies Eq. (60). By Eq. (53), one obtains

$$\begin{aligned} \mathbb{1} - \theta(\hat{N}_{\text{qp}}^{I_{p,j}}) &\xrightarrow{\nu^{-1}} \sum_{l \in I_{p,j}} (\mathbb{1} + Z_{p,l})/2 \\ &\xrightarrow{\nu^{-1}} \bigotimes_{l \in I_{p,j}} |0\rangle_{p,l} \langle 0|. \end{aligned} \quad (66)$$

and therefore

$$P_{\mathcal{I}} \xrightarrow{\nu^{-1}} \bigotimes_{p=1,2, l \in \cup_j I_{p,j}} |0\rangle_{p,l} \langle 0|. \quad (67)$$

Given that  $\cup_{p,j} I_{p,j} \cup \{\text{'parity'}\} = S_d$ ,

$$P_{\text{parity}} P_{\mathcal{I}} \xrightarrow{\nu^{-1}} \bigotimes_{r \in S_d} |0\rangle_r \langle 0| \xrightarrow{\nu} P_{\mathcal{S}}. \quad (68)$$

Therefore,  $P_{\text{parity}} P_{\mathcal{I}} = P_{\mathcal{S}}$ , which completes the proof.  $\square$

Theorem IV.3 implies that given a QP detector with inverse resolution  $\lambda$ , any error-detecting code  $\mathcal{C}_d$  with  $d \geq \lambda$  is implementable in such a way that any even total-parity error  $E$  that causes an undetected non-trivial logical operation has  $\text{wt}(E) \geq 4d + 4$ .

It is worthwhile to note that given a detector with resolution  $\lambda = 1$ , the code  $\mathcal{C}_0$  is not only error-detecting but also error-correcting. In this limit, QP detectors can implement all stabilizer measurements individually, and so the situation is analogous to the Kitaev tetron code. Any even total-parity error  $E$  with  $\text{wt}(E) \leq n - 1$  can be corrected by an appropriate (possibly linear) unitary operation on the MZMs. No operation on the bulk Majorana operators is required for the recovery operation. Unfortunately, this extraordinary capability cannot be achieved with QP detectors of inverse resolution  $\lambda \geq 2$ . Realizing this scenario requires a very high level of control over microscopic degrees of freedom, and therefore the investigation of this scenario, although very promising, is outside the scope of the present work.

#### D. Extension of error-detecting codes to parameters away from the fixed point

The observables  $\hat{N}_{\text{qp}}^I$  depend implicitly on the parameters  $(\mu, w, \Delta)$  of the system. Thus, if the Kitaev tetron is tuned away from the fixed point  $\mu = 0$  and  $w = \Delta = 1$ , the stabilizers defined in Eq. (21) are no longer directly accessible. It is nevertheless possible to construct error-detecting codes analogous to  $\mathcal{C}_d$  for arbitrary parameter values throughout the topological phase  $|\mu| < |w|$ .

The key observation is that the WQP operators satisfy the same commutation and anticommutation relations for any parameter values in the topological regime. Let  $\{\phi_j\}$  and  $\{\phi'_{j'}\}$  be the sets of WQP annihilators at two different parameter values  $(\mu, w, \Delta)$  and  $(\mu', w', \Delta')$  respectively. These satisfy the same canonical anticommutation rules:

$$\{\phi_j, \phi_{j'}^\dagger\} = \{\phi'_{j'}, (\phi'_{j'})^\dagger\} = \delta_{jj'} \mathbb{1}. \quad (69)$$

Therefore, the mapping in Eq. (53) is valid for all parameter values in the topological regime. New codes  $\mathcal{C}_d(\mu, w, \Delta)$  can then be constructed in exactly the same way as the  $\mathcal{C}_d$  were constructed at the fixed point.

The newly constructed codes  $\mathcal{C}_d(\mu, w, \Delta)$  have stabilizer operators of the form

$$Q_{p,l}(\mu, w, \Delta) = (-1)^{(\phi'_{p,l})^\dagger \phi'_{p,l}}, \quad (70)$$

which are exponentially localized in space, but not as compactly as at the fixed point. Lemma IV.1, Definition IV.2 and Theorem IV.3 follow as long as the weight  $\text{wt}'$  of the errors are defined in terms of WQPs. Consequently, the codes  $\mathcal{C}_d(\mu, w, \Delta)$  are error-detecting codes for errors that are local in the WQP basis. Note that the errors that are local in the original basis  $\{a_j^\dagger, a_j\}$  are not necessarily local in the WQP basis; however, due to exponential localization of WQPs, the overlap of a low- $\text{wt}'$  error on a high- $\text{wt}'$  error is exponentially small. For example, the overlap of an error with constant  $\text{wt}'$  on an error  $E$  with  $\text{wt}(E) \geq 4d + 4$  is exponentially small in  $d$ . This implies that an error with constant  $\text{wt}'$  can be

detected with probability  $1 - p_{\text{fail}}$ , where  $p_{\text{fail}}$  is exponentially small in  $d$ . One may therefore think of  $\mathcal{C}_d(\mu, w, \Delta)$  as an approximate error-detecting code with respect to low- $\text{wt}$  errors.

## V. QUANTIFYING THE ADVANTAGE OFFERED BY QUASIPARTICLE DETECTION

In this section, we compare the performance of qubits encoded in a Kitaev tetron with and without QP detection, in the presence of QP poisoning events. Having shown that the code  $\mathcal{C}_d$  can be implemented by using a detector with  $\lambda \leq d$ , it suffices to compare the performance of the codes  $\{\mathcal{C}_d\}$  against each other. The metric that we use for this comparison is the bit-flip error rate  $p_{\text{bit-flip}}$  and the erasure rate  $p_{\text{erasure}}$  for the logical qubit encoded in  $\mathcal{C}_d$ .

### A. The noise model

Assume a noise model where the system undergoes the channel

$$\rho \mapsto \mathcal{E}(\rho) = \mathcal{E}_{2,n} \circ \dots \mathcal{E}_{2,1} \circ \mathcal{E}_{1,n} \circ \dots \circ \mathcal{E}_{1,1}(\rho), \quad (71)$$

where

$$\mathcal{E}_{p,j}(\rho) = q(-ic_{2j-1}c_{2j})\rho(-ic_{2j-1}c_{2j}) + (1 - q)\mathbb{1} \quad (72)$$

for some  $q \in [0, 1]$ . The error channel  $\mathcal{E}_{p,j}$  implements the elementary error operator  $E_{p,j}$  – c.f. Eq. (24) – with probability  $q$ , and all elementary errors are independent. Therefore, for every  $\mathcal{J}_1, \mathcal{J}_2 \subseteq \{1, \dots, n\}$ , the error channel in Eq. (71) implements the error operator

$$E(\mathcal{J}_1, \mathcal{J}_2) = \prod_{p=1,2} \prod_{j \in \mathcal{J}_p} E_{p,j} \quad (73)$$

with probability

$$\text{prob}(\mathcal{J}_1, \mathcal{J}_2) = q^{|\mathcal{J}_1 + \mathcal{J}_2|} (1 - q)^{2n - |\mathcal{J}_1 + \mathcal{J}_2|}. \quad (74)$$

It is straightforward to verify that

$$\sum_{\mathcal{J}_1 \subseteq \{1, \dots, n\}} \sum_{\mathcal{J}_2 \subseteq \{1, \dots, n\}} \text{prob}(\mathcal{J}_1, \mathcal{J}_2) = 1, \quad (75)$$

so that the channel in Eq. (71) is both trace-preserving and completely positive owing to the Kraus form. At the fixed point,  $E_{p,j}$  for  $j \neq 1, n$  excites or de-excites two QPs with probability  $q$ . Therefore,  $q$  is roughly twice the rate of QP excitations per unit time per unit length, and is assumed to be independent of  $n$ . For  $j \in \{1, n\}$ , the error operator  $E_{p,j}$  excites or de-excites, with probability  $q$ , one QP above bulk energy gap while also acting on the adjacent MZM, which leads to QP poisoning. Consequently,  $q$  can also be interpreted as the rate of QP poisoning per MZM. The rate of relaxation of excited QPs

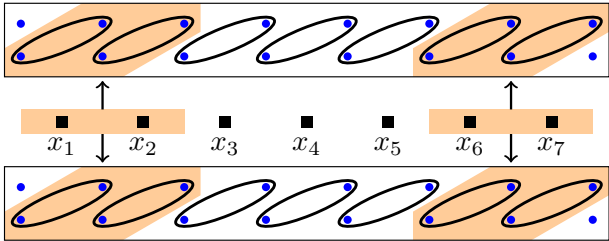


FIG. 6. The region under detection for implementing  $\mathcal{C}_2$  using a detector with inverse resolution  $\lambda = 2$  on a tetron of length  $n = 8$ .

is the same as the rate of excitation in this model, so this model mimics the noise due to coupling to a thermal bath at a very high temperature.

A couple of attributes of the noise model deserve a justification here. First, the noise model does not account for excited QPs spreading due to dispersion. Such an effect is present in any model of a topological superconductor away from the fixed point. The noise model effectively assumes that the rate of QP detection is high compared to the time required for QPs to escape the region of detection. This assumption keeps the analysis simple and provides a proof-of-principle demonstration of the erasure conversion scheme.

Second, the noise modelled by Eq. (71) preserves total fermion parity. In fact, the erasure conversion scheme is incapable of detecting local errors that are linear combinations of MZMs. The latter kind of errors are caused by extrinsic QP poisoning processes, in which a fermion is injected into the system from its environment. Nevertheless, such errors can often be suppressed by tuning some hardware parameters. For example, in nanowire-based implementations, a high charging energy for the superconducting island prohibits isolated electrons from hopping onto the nanowire from the neighboring quantum dots [28]. The residual linear errors can be corrected by the error-correcting code in the layer above the error-detecting code. It is worth a remark that while the errors considered here preserve the total parity, they do not necessarily preserve the Majorana parity  $\langle Q_{\text{parity}} \rangle$ . Consider, for instance, the error  $c_{1,1}c_{1,2} = \gamma_1c_{1,2}$  at the fixed point. This error is evidently bilinear and therefore has even total parity. However, in a low energy model, this same error is equivalently described by the linear operator  $\gamma_1$ , as all bulk degrees of freedom are traced out, and therefore has odd Majorana parity. This is the reason why it is crucial for most other works on Majorana codes to consider errors of both odd and even (Majorana) parity [15, 16], whereas it suffices for this work to only consider errors of even total parity.

## B. Error rates at the fixed point

The calculation of error rates at the fixed point is tractable because the error operators act locally on stabilizers, with which they either commute or anticommute. Suppose the qubit is initialized in the  $|\bar{0}\rangle \in \mathcal{F}_{2n}$  state of the codespace  $\mathcal{C}_d$ , where  $d \in \{0, \dots, \lfloor n/2 \rfloor - 1\}$ . Consider first the the rate of erasure  $p_{\text{erasure}}$ . Recall that the logical qubit will be erased and reset during decoding if either the QP detection or the MZM parity measurement signals an error. It is simpler to calculate the rate  $1 - p_{\text{erasure}}$ , which equals the probability of neither the QP detectors nor the MZM-parity measurement signaling an error. Suppose  $E(\mathcal{J}_1, \mathcal{J}_2)$  includes some Majorana operators and excludes at least one Majorana operator other than the MZM in a single detection region, say  $I_{1,1}$  (see Fig. 6). Then there exists at least one stabilizer  $Q_{p,l}$  with support on one excluded and one included Majorana operator, and therefore  $\langle Q_{p,l} \rangle = -1$ . Recall that a flipped stabilizer is equivalent to the presence of a QP, and therefore the QP detector monitoring the  $I_{1,1}$  region would click and subsequently the qubit will be erased. If the only excluded Majorana operator is the MZM in that detection region, then no  $Q_{p,l}$  would click. However, if  $E(\mathcal{J}_1, \mathcal{J}_2)$  includes an odd number of MZMs, then the MZM-parity measurement signals an error, and qubit will be erased again. One therefore concludes that the qubit is not erased only if the error operator  $E(\mathcal{J}_1, \mathcal{J}_2)$  includes all Majorana operators in zero, two or all four detection regions in  $\mathcal{I} = \{I_{1,1}, I_{1,2}, I_{2,1}, I_{2,2}\}$ .

The probability of  $E(\mathcal{J}_1, \mathcal{J}_2)$  including no Majorana operators in any of the four detection regions is  $(1 - q)^{4d+4}$ . This is because each detection region has overlap with  $d + 1$  elementary errors, and the probability of each elementary error not occurring is  $1 - q$ . Similarly, the probability of  $E(\mathcal{J}_1, \mathcal{J}_2)$ , including all Majorana operators in all four detection regions, is  $q^{4d+4}$ . Finally, the probability of  $E(\mathcal{J}_1, \mathcal{J}_2)$  including all Majorana operators in two out of four detection regions is  $6q^{2d+2}(1 - q)^{2d+2}$ , where the factor of 6 comes from the six ways of choosing two detection regions out of four. Adding all these probabilities, one obtains

$$1 - p_{\text{erasure}} = (1 - q)^{4d+4} + 6q^{2d+2}(1 - q)^{2d+2} + q^{4d+4}. \quad (76)$$

Consider second the bit-flip error rate  $p_{\text{bit-flip}}$ . This is defined to be the probability of a qubit initialized in the state  $|\bar{0}\rangle$  undergoing a bit flip conditional on it not being erased. A bit-flip error occurs if the error operator  $E(\mathcal{J}_1, \mathcal{J}_2)$  has support on exactly one MZM in each of the sets  $\{\gamma_1, \gamma_2\}$  and  $\{\gamma_3, \gamma_4\}$ . Such a bit-flip error goes undetected if  $E(\mathcal{J}_1, \mathcal{J}_2)$  includes all Majorana operators in an even number of detection regions, as explained in the previous paragraph. Both these conditions are satisfied if  $E(\mathcal{J}_1, \mathcal{J}_2)$  includes all Majorana operators in one region on  $p = 1$  chain and one region on  $p = 2$  chain. Therefore, the logical bit-flip error probability conditional on detection of errors, which is the logical bit-flip error rate,

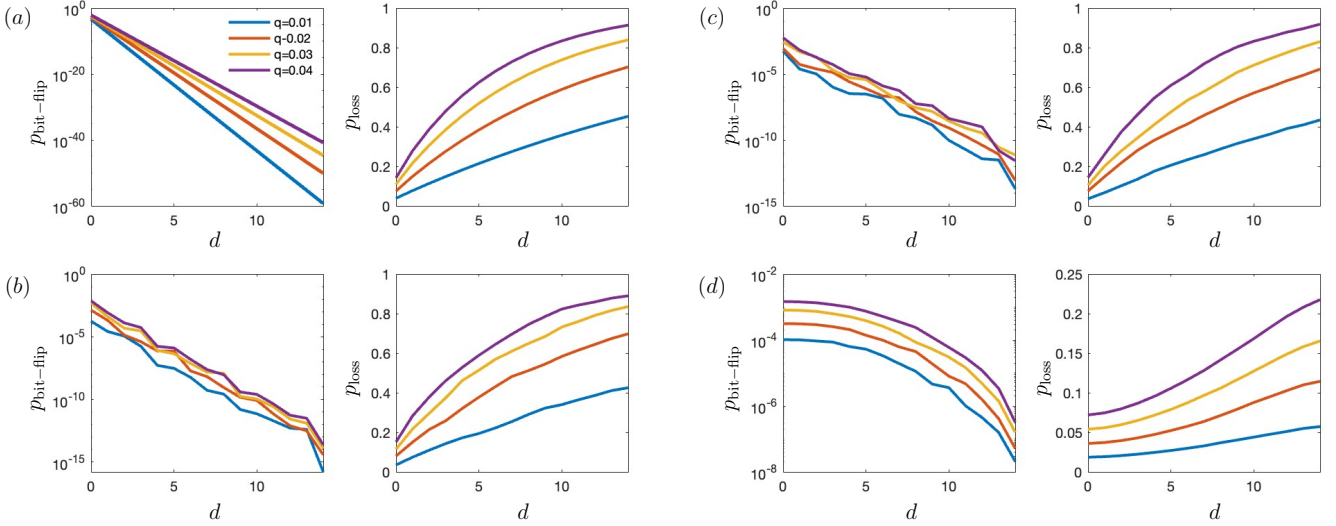


FIG. 7. Bit-flip rate (left column) and erasure rate (right column) as a function of  $d$  for various values of noise strength  $q$  at (a) the fixed point, i.e.  $\mu = 0$ ,  $w = 1$ ,  $\Delta = 1$ , (b) away from the fixed point at  $\mu = 0.3$ ,  $w = 1$ ,  $\Delta = 0.4$ ,  $n = 30$ , (c) with uniform on-site disorder of strength  $\delta\mu = 0.3$  at the same parameter values, and (d) near the topological phase boundary at  $\mu = 0.99$ ,  $w = 1$ ,  $\Delta = 0.1$ ,  $n = 30$ .

is

$$p_{\text{bit-flip}} = \frac{4q^{2d+2}(1-q)^{2d+2}}{(1-q)^{4d+4} + 6q^{2d+2}(1-q)^{2d+2} + q^{4d+4}}. \quad (77)$$

Here the denominator is simply the probability of the qubit not being lost, which is  $1 - p_{\text{erasure}}$  calculated in Eq. (76). Note that both the erasure rate as well as the bit-flip error rate are independent of  $n$  at the fixed point.

The error rates at the fixed point, Eqs. (76) and (77), are plotted in Fig. 7(a). Focus on the parameter regime  $q \ll 1/d \ll 1$ , which requires QP detectors with spatial resolution higher than the density of QPs excited by noisy operations. In this regime, the erasure probability scales as  $p_{\text{erasure}} \sim (4d + 4)q$ , i.e. increases linearly in the code distance, while the bit-flip probability scales as  $p_{\text{bit-flip}} \sim 4q^{2d+2}$ , i.e. decreases exponentially with the code distance. QP detection therefore allows trading off a significant fraction of Pauli errors for erasure errors. If  $d$  is chosen too high, then  $p_{\text{erasure}} \approx 1$ . A critical value of  $d$  is likely to be the most advantageous, and will depend on the error-correction scheme in use. Assuming access to arbitrarily high resolution, suppose the error-correction scheme tolerates a constant  $p_{\text{erasure}}$ . In terms of the erasure rate, one can express the bit-flip error rate as

$$p_{\text{bit-flip}} \approx 4q^{(p_{\text{erasure}}/4q)}. \quad (78)$$

Therefore,  $p_{\text{bit-flip}}$  is suppressed exponentially in  $1/q$  for fixed  $p_{\text{erasure}}$ . Equation (78) shows a glimpse of why QP detection could be extremely powerful for achieving fault tolerance and for reducing resource overhead imposed by error correction.

### C. Error rates away from the fixed point

#### 1. Formalism

If the Kitaev tetron is tuned to parameters away from the fixed point, then the error rates are not tractable analytically. Results are instead obtained numerically using the covariance matrix framework, and the basis defined by Wannier QPs makes the calculation considerably simpler. Define Majorana operators  $\{c'_j, j = 1, \dots, 2n\}$  using the relations

$$\begin{aligned} \phi_{p,l}^\dagger &= (c'_{p,2l} + ic'_{p,2l+1})/2, & \phi_{p,l} &= (c'_{p,2l} - ic'_{p,2l+1})/2, \\ \gamma_1 &= c'_{1,1}, & \gamma_2 &= c'_{1,2n}, & \gamma_3 &= c'_{2,1}, & \gamma_4 &= c'_{2,2n}. \end{aligned} \quad (79)$$

The covariance matrix  $M_0$  of  $|\bar{0}\rangle$  is defined with respect to  $\{c'_{p,j}, p = 1, 2, j = 1, \dots, 2n\}$ , c.f. Lemma II.2. The erasure rate after the state has been subjected to  $\mathcal{E}$  is given by

$$p_{\text{erasure}} = 1 - \langle P_S \rangle_{\mathcal{E}(\rho)} = 1 - \left\langle \prod_{r \in S_d} \frac{(\mathbb{1} + Q_r)}{2} \right\rangle_{\mathcal{E}(\rho)}. \quad (80)$$

The expectation value is obtained by first sampling an error operator  $E$ , which is performed by independently sampling two strings in  $\{0, 1\}^n$  from the probability distribution  $\{q, 1-q\}^{\times n}$ . Let  $\mathcal{J}_1, \mathcal{J}_2$  be the sets of positions of 1s in the two strings respectively. The corresponding error operator  $E(\mathcal{J}_1, \mathcal{J}_2)$  is given by Eq. (73). The normalized state after the action of  $E$  is  $E|\bar{0}\rangle / \|E|\bar{0}\rangle\|$ . To calculate the covariance matrix of  $E|\bar{0}\rangle$ ,  $E$  is expressed as a unitary operator generated by a quadratic Hamiltonian, as follows.

**Lemma V.1.** *The following identity holds:*

$$\prod_{p=1,2} \prod_{j \in \mathcal{J}_p} E_{p,j} = i^{|\mathcal{J}_1 + \mathcal{J}_2|} \exp \left( -\frac{i\pi}{2} \sum_{p=1,2} \sum_{j \in \mathcal{J}_p} E_{p,j} \right). \quad (81)$$

With this lemma, one can write  $M_{E|\bar{0}\rangle} = R_s M_0 R_s^T$ , where

$$R_s = \exp \left[ \frac{\pi}{2} \sum_{j \in s} (|2j-1\rangle \langle 2j| - \text{H.c.}) \right]. \quad (82)$$

The matrix elements of the effective Hamiltonian  $i(\sum_{j \in s} |2j-1\rangle \langle 2j| - \text{H.c.})$  are computed in the WQP basis in order to obtain the matrix representation of  $R_s$ , which in turn generates  $M_{E|\bar{0}\rangle}$ . Finally, to calculate  $p_{\text{erasure}}$  corresponding to  $E$ , the following lemmas are used:

**Lemma V.2.** *The projector on the +1 eigenspace of  $Q_{p,l}$  is*

$$P_{p,l} = \frac{(\mathbb{1} + Q_{p,l})}{2} = \frac{c_{p,2l}(c_{p,2l} - ic_{p,2l+1})}{2}. \quad (83)$$

**Lemma V.3.** *For  $P_{\text{parity}} = (\mathbb{1} + (-i\gamma_1\gamma_2)(-i\gamma_3\gamma_4))/2$ ,*

$$P_{\text{parity}}(-i\gamma_1\gamma_2)P_{\text{parity}} = -i\gamma_1\gamma_2 - i\gamma_3\gamma_4. \quad (84)$$

The bit-flip error rate is defined to be

$$p_{\text{bit-flip}} = (1 - \langle \bar{Z} \rangle)/2, \quad \langle \bar{Z} \rangle = \frac{\langle P_S(-i\gamma_1\gamma_2)P_S \rangle_{\mathcal{E}(\rho)}}{\langle P_S \rangle_{\mathcal{E}(\rho)}}, \quad (85)$$

which can be calculated using similar techniques. The numerator of  $\bar{Z}$  is computed using Lemmas V.2 and V.3.

## 2. Results

For parameters away from the fixed point, noise can induce errors due to the overlap of MZMs. Also, now elementary errors have non-zero overlap on spatially distant stabilizers, which results in a larger fraction of high-weight errors, and consequently a larger fraction of undetected logical errors. The erasure and bit-flip error rates as a function of  $q$  are plotted in Fig. 7(b) for parameters away from the fixed point but nevertheless away from the topological phase boundary. The qualitative behaviors are similar to those at the fixed point and one observes a clear trade-off between Pauli and erasure errors. Consequently, a critical value of  $d$  is likely to be the most advantageous, as was inferred from the analysis at the fixed point. The qualitative behavior of error rates also remains the same in the presence of weak disorder, Fig. 7(c). However, the absolute rate of bit-flip errors in both Fig. 7(b) and Fig. 7(c) is higher than at the fixed point, as one would expect due to higher overlap of Majorana modes with distant WQPs. Such a comparison of

absolute error rates across parameter values is somewhat unfair, though, as the noise strength  $q$  is assumed to be independent of the parameter values. In real systems, the noise strength is likely to be higher for systems with parameters that lead to a low bulk energy gap.

The behaviors of the erasure and bit-flip errors change as the parameters approach the topological phase boundary, Fig. 7(d), because of the increased spatial extent of both the MZMs and the WQPs (for the latter refer to Fig. 3). Consequently, a local error can induce coherence between a MZM and a distant WQP. Nevertheless, the Pauli error rates continue to be exponentially suppressed as long as  $d$  is much larger than the characteristic length of the MZMs and the WQPs, both of which increase as the many-body gap decreases. This constrains the domain of  $q$  over which Pauli error decrease exponentially, because this behavior is expected to hold only for  $q \ll 1/d$ . For a constant QP poisoning rate  $q$ , the effective erasure rate is smaller in magnitude at fixed  $d$  as the parameters approach the topological phase boundary. The origin of this effect can be traced to fermionic interference effects arising from the fact that the QP basis is nearly conjugate to the basis in which errors are local.

It is worth emphasizing that the exponential suppression of Pauli error rates is a direct consequence of the exponential localization of WQPs. Consider the error operator  $E_{1,1}E_{2,1} = -c_{1,1}c_{1,2}c_{2,1}c_{2,2}$ . At the fixed point, this error is not detected by the stabilizer  $Q_{\text{parity}}$  because it involves two MZMs, namely  $\gamma_1 = c_{1,1}$  and  $\gamma_3 = c_{2,1}$ , but it is detected by QP detectors as long as  $d \geq 1$ . If the same error occurs on a tetron with parameters away from the fixed point, it may go undetected by both  $Q_{\text{parity}}$  and the QP detectors with some non-zero probability  $p_{\text{fail}}$ . The probability  $p_{\text{fail}}$  is proportional to the overlap of the error with the WQP operators supported in the region not under detection. Due to exponential localization of WQPs,  $p_{\text{fail}}$  is exponentially small in  $d$ , which in turn accounts for the exponential suppression of the Pauli error rate.

The error rates for logical qubits discussed above are only meaningful if it is assumed that  $\mathcal{C}_d$  constitutes the first layer of a concatenated error-correcting code. In that case, the qubits encoded in  $\mathcal{C}_d$  in individual Kitaev tetrtons are considered as the physical qubits for the next layer of error correction, and not as the logical qubits per se. Suppose that QP detection is performed in parallel with MZM parity measurement on each tetron, and both these measurements are perfect. If either of the QP or the MZM parity detectors signal an error, then the state is unrecoverable; the qubit is then discarded and subsequently reset during the decoding protocol of the concatenated code. In this setting, the error rates for the logical qubit encoded in  $\mathcal{C}_d$  would be treated as physical error rates for the next layer of the concatenated code. The threshold rates for erasure and Pauli errors respectively could then be calculated; these would depend, in general, on the details of the upper layers of

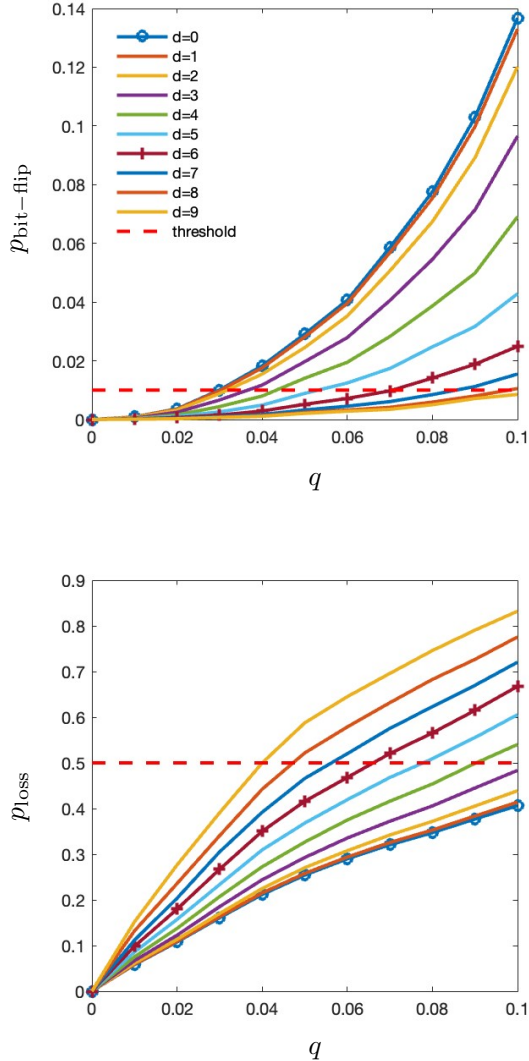


FIG. 8. Bit-flip error rate (top) and erasure rate (bottom) as a function of the noise strength  $q$  for various values of  $d$  at  $\mu = 0.95$ ,  $w = 1$ ,  $\Delta = 0.05$  and  $n = 30$ . The blue curves with ‘o’ markers correspond to error rates with no QP detection ( $d = 0$ ), and the maroon curves with ‘+’ markers correspond to  $d = 6$ . The red dashed curves indicate typical threshold values for the respective error rates.

the concatenated code. The implementation of such a concatenated code for any value of  $d$  requires the same number of tetrons and the same amount of time per cycle, allowing for a fair comparison.

Figure 8 depicts the erasure and Pauli error rates as a function of  $q$  for various values of  $d$  for parameters away from the fixed point and far from the topological phase boundary; the rates for  $d = 0$  correspond to no QP detection. The trade-off between Pauli and erasure rates is clearly seen, as the bit-flip error rate decreases and

the erasure rate increases with  $d$ . Assume that a second layer of quantum error-correcting code above  $\mathcal{C}_d$  has a threshold rate of 1% for Pauli errors and 50% for erasure errors, values consistent with thresholds for topological codes [24, 25]. For  $d = 0$ , i.e. without QP detection, the bit-flip error rate is above the typical threshold for  $q > q_{\text{th}}^{(0)} \approx 0.03$ . The erasure rate is well below the typical threshold for  $q < q_{\text{th}}^{(0)}$ . Therefore, for the parameters chosen in Fig. 8, fault-tolerance can be achieved without QP detection for  $q < q_{\text{th}}^{(0)} \approx 0.03$ . In comparison, if  $\mathcal{C}_6$  is used for the first layer of the error-correcting code, then fault-tolerance can be achieved for  $q < q_{\text{th}}^{(6)} \approx 0.06$ . Since  $q_{\text{th}}^{(6)} > q_{\text{th}}^{(0)}$ , the concatenated error-correcting code can tolerate higher rate of QP poisoning errors with QP detection in the first layer. Note that a detector with spatial resolution  $\lambda \leq 6$  allows for the implementation of  $d = 6$ , and therefore achieves the threshold value  $q_{\text{th}}^{(6)}$ . For  $d > 6$ , the threshold rate  $q_{\text{th}}^{(d)}$  is limited by the erasure rate and therefore drops below  $q_{\text{th}}^{(6)}$ . Therefore,  $d = 6$  is optimal if  $q_{\text{th}}^{(d)}$  is the figure of merit and only requirements are  $p_{\text{bit-flip}} < 0.01$  and  $p_{\text{erasure}} < 0.5$ .

Note that the precise values of  $q_{\text{th}}$  are not practically important as the noise model considered here is not tied to specific implementations. Likewise, a concatenated quantum error correcting code with a topological code in the outer layer may not be feasible or optimal for realistic tetron architectures. Considering its high threshold rate [15, 16], the Majorana surface code modified to leverage QP detection measurements might be a better alternative than a concatenated code as considered above. Regardless, the numerical results above demonstrate that QP detection could be highly advantageous for achieving fault tolerance and for reducing the resource cost incurred by error correction.

## VI. CONCLUSIONS

The problem addressed in this work is to ascertain to what extent a spatially resolved detection of QPs can aid in improving the quality of topological qubits, encoded in MZMs. A model of QP detection with finite spatial resolution is proposed, via the construction of a suitable QP position operator. The eigenmodes of the QP position operator, which describe the WQPs, are proven to be exponentially localized. Majorana error-detecting codes are then designed that can be implemented on a tetron with the help of QP detection. These codes facilitate erasure conversion by detecting local QP poisoning errors. Finally, assuming that the dominant errors arise from intrinsic QP poisoning, we have shown that the resulting erasure conversion scheme suppresses the Pauli error rates exponentially in the code distance, at the cost of a linearly increasing erasure rate. This exponential suppression is tied to the exponential localization of WQPs. While our analysis is done entirely on the Kitaev tetron

model, it can be easily extended to tetrons based on other models of topological superconductors, and so we expect an exponential suppression in Pauli error rate in those cases as well. Thus, QP detection allows to remove a large fraction of Pauli errors at the cost of increased erasure errors, which are easier to correct in a second layer of a concatenated quantum error-correcting code. Therefore, QP detection is an appealing approach for tackling intrinsic QP poisoning errors in Majorana qubits, and thereby achieve fault tolerance.

Most important, QP detection bolsters the passive protection that is inherent to topological systems such as those that support MZMs considered here. As mentioned previously, the errors that are dominated by the overlap of the computational anyons, and are not mediated by QP poisoning, are suppressed exponentially in the distance between the computational anyons. Therefore, such errors can be suppressed by increasing the distance between anyons. However, the errors arising from QP poisoning are suppressed only in the bulk energy gap, which is not easy to tune in experiments [12, 37–42]. Our results show that QP detectors with spatial resolution can be effective in suppressing these QP poisoning errors.

Several questions remain to be answered in this context. One is how best to implement the position-resolving QP detector modeled in our work in practical Majorana-based qubits. Because the QP detection region in our scheme overlaps with the MZMs, the main challenge is to detect QPs without destroying the information stored in MZMs. A potential approach would be to leverage the energy separation between the MZMs and the bulk QPs for this purpose. However, no experimental measurement is known to our knowledge that can probe high-energy QPs without coupling to MZMs. Therefore, implementation of QP detection near the ends of the tetron as modeled in this work requires further research. Meanwhile, one may perform erasure conversion sufficiently far from the MZMs so as to reduce disturbance to the MZMs. While such detectors are likely to be less effective for erasure conversion than the ones modeled in this work, they may nevertheless lead to improved threshold QP poisoning rate.

Another question is how quickly one must perform QP detection measurements in practice, to ensure that the QP remains localized. A good estimate can be obtained by considering that the QPs must not escape the detection region in time  $\Delta t$  between two successive measurements. To obtain a quantitative estimate, consider Majorana qubits of semiconductor nanowires. These are proposed to be tens of micrometers in length [43], so assume a detection region of approximately  $1 \mu\text{m}$ . The average QP speed in thermal equilibrium is given by  $\langle |v_{\text{qp}}| \rangle \sim v_F \sqrt{1/\beta\Delta}$  where  $v_F$  is the Fermi velocity,  $\beta$  is the inverse temperature and  $\Delta$  is the induced superconducting gap (see Appendix D). Using typical values  $\beta\Delta \sim 100$

and  $v_F \sim 10^5 \text{ m/s}$ , one obtains  $\langle |v_{\text{qp}}| \rangle \sim 10^4 \text{ m/s}$  and  $\Delta t \sim 0.1 \text{ ns}$ . While challenging, these measurement timescales are currently achievable in semiconductor tunnel junction experiments [44], and nanosecond timescales have been achieved in time-resolved transport measurements [45]. Furthermore, a significantly higher  $\Delta t$  could suffice if the quasiparticles relax to the lower band edge due to inelastic scattering processes, if the chemical potential is set to a value with lower Fermi velocity  $v_F$ , and if a higher topological band gap could be achieved.

Another challenge is to devise optimal schemes for leveraging QP detection in practical applications, including those beyond Majorana-based quantum computation. In Majorana-based architectures, the obvious next step is to develop decoding strategies for the Majorana surface code and its variants that leverage QP detection measurements. A strategy similar to the ones for tackling erasure in qubit surface code [24, 25] is likely to succeed. For other topological platforms such as those based on fractional quantum Hall states [1], a theoretical formalism for QP detection needs to be developed. In Majorana tetrons, constructing a QP detection operator was relatively straightforward, as Eq. (7) is quadratic in field operators; equivalently, the effective (mean-field) Hamiltonian is non-interacting. Modeling QP detection in other systems is a problem of interest for topological quantum computation in general and also for fundamental physics. Similarly, the exponential localization of the WQP operators requires only that the many-body system has a bulk energy gap that remains open in the thermodynamic limit. The WQPs in Majorana tetrons can be used, in principle, to detect errors mainly because any even-parity error that acts on a MZM affects the state of a QP. It remains to be investigated if an analogous construction exists in other topological phases characterized by gapless surface modes, for example in fractional quantum Hall states. On the quantum error correction front, our work motivates inquiry into the practical implementation of active quantum error correction given limited control, and finite detector resolution, of the microscopic degrees of freedom.

## ACKNOWLEDGMENTS

This research was supported by the Natural Sciences and Engineering Research Council of Canada, the Alberta Major Innovation Fund and the Australian Research Council Centre of Excellence for Engineered Quantum Systems (CE170100009). A.A. acknowledges support by Killam Trusts (Postdoctoral Fellowship). K.D.S. acknowledge support by the Simons Foundation (Postdoctoral Fellowship). A.A. is grateful for insightful conversations with Salini Karuvade, Susan Coppersmith, Dominic Williamson, Andrew C. Doherty and Stephen Bartlett.

---

[1] C. Nayak, S. H. Simon, A. Stern, M. Freedman, and S. Das Sarma, Non-Abelian anyons and topological quantum computation, *Rev. Mod. Phys.* **80**, 1083 (2008).

[2] A. Y. Kitaev, Unpaired Majorana fermions in quantum wires, *Phys.-Usp.* **44**, 131 (2001).

[3] A. Y. Kitaev, Fault-tolerant quantum computation by anyons, *Ann. Phys. (N. Y.)* **303**, 2 (2003).

[4] M. Freedman, A. Kitaev, M. Larsen, and Z. Wang, Topological quantum computation, *Bull. Amer. Math. Soc.* **40**, 31 (2003).

[5] S. Bravyi and R. König, Disorder-assisted error correction in Majorana chains, *Commun. Math. Phys.* **316**, 641 (2012).

[6] E. Dennis, A. Kitaev, A. Landahl, and J. Preskill, Topological quantum memory, *J. Math. Phys.* **43**, 4452 (2002).

[7] F. Pastawski, A. Kay, N. Schuch, and I. Cirac, Limitations of passive protection of quantum information, *Quantum Inf. Comput.* **10**, 580–618 (2010).

[8] T. Karzig, W. S. Cole, and D. I. Pikulin, Quasiparticle poisoning of Majorana qubits, *Phys. Rev. Lett.* **126**, 057702 (2021).

[9] R. V. Mishmash, B. Bauer, F. von Oppen, and J. Alicea, Dephasing and leakage dynamics of noisy Majorana-based qubits: Topological versus Andreev, *Phys. Rev. B* **101**, 075404 (2020).

[10] S. D. Sarma, M. Freedman, and C. Nayak, Majorana zero modes and topological quantum computation, *npj Quantum Inf.* **1**, 15001 (2015).

[11] C. Knapp, T. Karzig, R. M. Lutchyn, and C. Nayak, Dephasing of Majorana-based qubits, *Phys. Rev. B* **97**, 125404 (2018).

[12] D. Rainis and D. Loss, Majorana qubit decoherence by quasiparticle poisoning, *Phys. Rev. B* **85**, 174533 (2012).

[13] C. Knapp, M. Beverland, D. I. Pikulin, and T. Karzig, Modeling noise and error correction for Majorana-based quantum computing, *Quantum* **2**, 88 (2018).

[14] G. Dauphinais and D. Poulin, Fault-tolerant quantum error correction for non-Abelian anyons, *Commun. Math. Phys.* **355**, 519 (2017).

[15] S. Vijay, T. H. Hsieh, and L. Fu, Majorana fermion surface code for universal quantum computation, *Phys. Rev. X* **5**, 041038 (2015).

[16] C. McLauchlan and B. Béri, A new twist on the Majorana surface code: Bosonic and fermionic defects for fault-tolerant quantum computation, *Quantum* **8**, 1400 (2024).

[17] S. Bravyi, B. M. Terhal, and B. Leemhuis, Majorana fermion codes, *New J. Phys.* **12**, 083039 (2010).

[18] K. S. Chou, T. Shemella, H. McCarrick, *et al.*, A superconducting dual-rail cavity qubit with erasure-detected logical measurements, *Nat. Phys.* **20**, 1454 (2024).

[19] H. Levine, A. Haim, J. S. C. Hung, *et al.*, Demonstrating a long-coherence dual-rail erasure qubit using tunable transmons, *Phys. Rev. X* **14**, 011051 (2024).

[20] Y. Wu, S. Kolkowitz, S. Puri, and J. D. Thompson, Erasure conversion for fault-tolerant quantum computing in alkaline earth rydberg atom arrays, *Nature Communications* **13**, 4657 (2022).

[21] M. Kang, W. C. Campbell, and K. R. Brown, Quantum error correction with metastable states of trapped ions using erasure conversion, *PRX Quantum* **4**, 020358 (2023).

[22] S. Kivelson, Wannier functions in one-dimensional disordered systems: Application to fractionally charged solitons, *Phys. Rev. B* **26**, 4269 (1982).

[23] M. B. Hastings and X.-G. Wen, Quasiadiabatic continuation of quantum states: The stability of topological ground-state degeneracy and emergent gauge invariance, *Phys. Rev. B* **72**, 045141 (2005).

[24] T. M. Stace, S. D. Barrett, and A. C. Doherty, Thresholds for topological codes in the presence of loss, *Phys. Rev. Lett.* **102**, 200501 (2009).

[25] T. M. Stace and S. D. Barrett, Error correction and degeneracy in surface codes suffering loss, *Phys. Rev. A* **81**, 022317 (2010).

[26] J. P. Blaizot and G. Ripka, *Quantum theory of finite systems* (MIT press, Cambridge (MA), 1986).

[27] A. Alase, E. Cobanera, G. Ortiz, and L. Viola, Exact solution of quadratic fermionic Hamiltonians for arbitrary boundary conditions, *Phys. Rev. Lett.* **117**, 076804 (2016).

[28] T. Karzig *et al.*, Scalable designs for quasiparticle-poisoning-protected topological quantum computation with Majorana zero modes, *Phys. Rev. B* **95**, 235305 (2017).

[29] T. B. Smith, M. C. Cassidy, D. J. Reilly, S. D. Bartlett, and A. L. Grimsmo, Dispersive readout of Majorana qubits, *PRX Quantum* **1**, 020313 (2020).

[30] H.-L. Lai and W.-M. Zhang, Decoherence dynamics of Majorana qubits under braiding operations, *Phys. Rev. B* **101**, 195428 (2020).

[31] M. A. Nielsen and I. L. Chuang, *Quantum Computation and Quantum Information: 10th Anniversary Edition* (Cambridge University Press, Cambridge, 2010).

[32] J. Surace and L. Tagliacozzo, Fermionic Gaussian states: An introduction to numerical approaches, *SciPost Phys. Lect. Notes* **54** (2022).

[33] P. Kok, W. J. Munro, K. Nemoto, T. C. Ralph, J. P. Dowling, and G. J. Milburn, Linear optical quantum computing with photonic qubits, *Rev. Mod. Phys.* **79**, 135 (2007).

[34] H. Bombín, Gauge color codes: optimal transversal gates and gauge fixing in topological stabilizer codes, *New J. Phys.* **17**, 083002 (2015).

[35] D. Poulin, Stabilizer formalism for operator quantum error correction, *Phys. Rev. Lett.* **95**, 230504 (2005).

[36] G. Dauphinais, D. W. Kribs, and M. Vasmer, Stabilizer formalism for operator algebra quantum error correction, *Quantum* **8**, 1261 (2024).

[37] G. Goldstein and C. Chamon, Decay rates for topological memories encoded with Majorana fermions, *Phys. Rev. B* **84**, 205109 (2011).

[38] J. C. Budich, S. Walter, and B. Trauzettel, Failure of protection of Majorana based qubits against decoherence, *Phys. Rev. B* **85**, 121405 (2012).

[39] L. Mazza, M. Rizzi, M. D. Lukin, and J. I. Cirac, Robustness of quantum memories based on Majorana zero modes, *Phys. Rev. B* **88**, 205142 (2013).

[40] Y. Hu, Z. Cai, M. A. Baranov, and P. Zoller, Majorana fermions in noisy Kitaev wires, *Phys. Rev. B* **92**, 165118 (2015).

[41] F. L. Pedrocchi, N. E. Bonesteel, and D. P. DiVincenzo, Monte Carlo studies of the self-correcting properties of

the Majorana quantum error correction code under braiding, *Phys. Rev. B* **92**, 115441 (2015).

[42] M. Ippoliti, M. Rizzi, V. Giovannetti, and L. Mazza, Quantum memories with zero-energy Majorana modes and experimental constraints, *Phys. Rev. A* **93**, 062325 (2016).

[43] M. Aghaee, A. Akkala, Z. Alam, *et al.* (Microsoft Quantum), Inas-al hybrid devices passing the topological gap protocol, *Phys. Rev. B* **107**, 245423 (2023).

[44] K. Liang, L. Bi, Q. Zhu, H. Zhou, and S. Li, Ultrafast dynamics revealed with time-resolved scanning tunneling microscopy: A review, *ACS Appl. Opt. Mater.* **1**, 924 (2023).

[45] H. Kamata, H. Irie, N. Kumada, and K. Muraki, Time-resolved measurement of ambipolar edge magneto-plasmon transport in InAs/InGaSb composite quantum wells, *Phys. Rev. Res.* **4**, 033214 (2022).

[46] L. Grafakos, *Classical Fourier Analysis*, Graduate Texts in Mathematics, Vol. 249 (Springer, New York, 2009).

[47] F. Kittaneh, Inequalities for commutators of positive operators, *J. Funct. Anal.* **250**, 132 (2007).

[48] Y.-Q. Wang and H.-K. Du, Norms of commutators of self-adjoint operators, *J. Math. Anal. Appl.* **342**, 747 (2008).

[49] J. Lu, K. D. Stubbs, and A. B. Watson, Existence and computation of generalized Wannier functions for non-periodic systems in two dimensions and higher, *Arch. Rational Mech. Anal.* **243**, 1269 (2022).

[50] M. Reed and B. Simon, *I: Functional analysis*, Vol. 1 (Gulf Professional Publishing, 1980).

[51] E. Guadagnini, Quasi-particles, thermodynamic consistency, and the gap equation, *Advances in Mathematical Physics* **2017**, 6265427 (2017).

## Appendix A: Properties of Exponentially Localized Operators

In this section, we provide some results on exponentially localized operators, which we later use for proving exponential localization of WQPs. We begin these technical estimates with a definition.

**Definition A.1.** We say an operator  $A$  on  $\ell^2(\mathbb{Z}^+ \times \mathbb{C}^D)$  is *exponentially localized operator* with rate  $\kappa > 0$  and prefactor  $C$  if

$$|\langle j, m | A | j', m \rangle| \leq C e^{-\kappa |j-j'|}. \quad (\text{A1})$$

Clearly, by definition, the Hamiltonian  $H$  is an exponentially localized operator and the main content of Lemma III.2 is to prove that  $P_{\text{qp}}$  is exponentially localized as well. Exponentially localized operators satisfy a number of important estimates which we will make great use of in our proofs.

The decay properties of exponentially localized operators are most easily expressed in terms of the exponential growth operator which depends on two real constants  $g, x$ :

$$B_{g,x} = \sum_{m,j} e^{g|j-x|} |j, m\rangle \langle j, m|. \quad (\text{A2})$$

In particular, exponentially localized operators have the following properties:

**Lemma A.2.** *If  $A$  is an exponentially localized operator with rate  $\kappa$  and prefactor  $C$  then*

1.  *$A$  is a bounded operator on  $\ell^2(\mathbb{Z}^+ \times \mathbb{C}^D)$ .*

2. *For all  $x \in \mathbb{R}$  and all  $0 \leq g \leq \frac{1}{2}\kappa$ ,*

$$\|B_{g,x} A B_{g,x}^{-1} - A\| \leq 8CD\kappa^{-2}g \quad (\text{A3})$$

3. *For all  $x \in \mathbb{R}$  and all  $0 \leq g \leq \frac{1}{2}\kappa$ ,*

$$\|[B_{g,x} A B_{g,x}^{-1}, \tilde{X}]_-\| \leq 8CD\kappa^{-2}, \quad (\text{A4})$$

where  $\tilde{X} = \sum_{m=1}^D \sum_j j |j, m\rangle \langle j, m|$ .

Note that  $\tilde{X} = NX$  for the Kitaev chain, see the proof of Thm. III.1.

**Remark A.3.** The restriction  $g \leq \frac{1}{2}\kappa$  is not strictly necessary.  $g$  may be chosen to be any value strictly less than  $\kappa$ . However, the prefactor becomes larger as  $|\kappa - g|$  becomes smaller.

The main technical lemma to prove Lemma A.2 will be Schur's lemma specialized for linear operators on  $\ell^2(\mathbb{Z}^+ \times \mathbb{C}^D)$ :

**Theorem A.4** (Schur's Lemma (Appendix I[46])). Suppose  $T$  is a linear operator on  $\ell^2(\mathbb{Z}^+ \times \mathbb{C}^D)$  of the form

$$T = \sum_{j,m} \sum_{j',m'} \langle j, m | T | j', m' \rangle |j, m\rangle \langle j', m'|. \quad (\text{A5})$$

That is  $T$  is a discrete integral operator (infinite matrix) on  $\ell^2(\mathbb{Z}^+ \times \mathbb{C}^D)$  with kernel function

$$K((j, m), (j', m')) := \langle j, m | T | j', m' \rangle. \quad \text{If}$$

$$\begin{aligned} B_0 &:= \sup_{j,m} \sum_{j',m'} |\langle j, m | T | j', m' \rangle|, \\ B_1 &:= \sup_{j',m'} \sum_{j,m} |\langle j, m | T | j', m' \rangle| \end{aligned} \quad (\text{A6})$$

are finite, then  $\|T\| \leq \sqrt{B_0 B_1}$ .

Here and henceforth,  $:=$  stands for definition.

*Proof of Lemma A.2.* We start by writing  $A$  in the position basis

$$A = \sum_{m,j} \sum_{m',j'} \langle j, m | A | j', m' \rangle |j', m'\rangle \langle j, m|. \quad (\text{A7})$$

To show  $A$  is bounded, following Schur's test, we first bound the “ $B_0$ ” constant by

$$\begin{aligned} \sup_{j,m} \sum_{m'=1}^D \sum_{j' \in \mathbb{Z}^+} |\langle j, m | A | j', m' \rangle| &\leq \sup_{j,m} \sum_{m'=1}^D \sum_{j' \in \mathbb{Z}^+} C e^{-\kappa |j-j'|} \\ &\leq \sup_j \sum_{j' \in \mathbb{Z}^+} C D e^{-\kappa |j-j'|} \\ &\leq \sup_j \int_{-\infty}^{\infty} C D e^{-\kappa |x-j|} dx \\ &\leq 2 C D \kappa^{-1}. \end{aligned} \quad (\text{A8})$$

Repeating the same steps for the “ $B_1$ ” constant in Schur's test, we find the same upper bound and hence  $\|A\| \leq C D \kappa^{-1}$ .

Now we proceed to show the bound for  $B_{g,x} A B_{g,x}^{-1} - A$ . Expanding this operator in the position basis we have:

$$B_{g,x} A B_{g,x}^{-1} - A = \sum_{m,j} \sum_{m',j'} \left( e^{g|j'-x|} e^{-g|x-j|} - 1 \right) \langle j, m | A | j', m' \rangle |j', m'\rangle \langle j, m| \quad (\text{A9})$$

Therefore, following Schur's test we consider

$$\sup_{j,m} \sum_{m'=1}^D \sum_{j' \in \mathbb{Z}^+} |\left( e^{g|j'-x|} e^{-g|x-j|} - 1 \right) \langle j, m | A | j', m' \rangle| \quad (\text{A10})$$

One can easily verify that for all  $g > 0$  and all  $j, j' \in \mathbb{Z}^+$

$$|e^{g(|j'-x|-|j-x|)} - 1| \leq |e^{g|j'-j|} - 1| \leq g|j-j'| e^{g|j'-j|} \quad (\text{A11})$$

Hence so long as  $g < \kappa$ :

$$\begin{aligned} \sup_{j,m} \sum_{m'=1}^D \sum_{j' \in \mathbb{Z}^+} |\left( e^{g|j'-x|} e^{-g|x-j|} - 1 \right) \langle j, m | A | j', m' \rangle| &\leq \sup_{j,m} \sum_{m'=1}^D \sum_{j' \in \mathbb{Z}^+} g|j-j'| e^{g|j'-j|} |\langle j, m | A | j', m' \rangle| \\ &\leq \sup_j \sum_{j' \in \mathbb{Z}^+} C g D |j-j'| e^{(g-\kappa)|j'-j|} \\ &\leq 2 C D g (\kappa - g)^{-2} \\ &\leq 8 C D g \kappa^{-2} \end{aligned} \quad (\text{A12})$$

where in the last line we have used that by assumption  $g \leq \frac{1}{2}\kappa$ . As before, a similar calculation shows that the “ $B_1$ ” term can be bounded by the same quantity. Hence,

$$\|B_{g,x} A B_{g,x}^{-1} - A\| \leq 8 C D \kappa^{-2} g. \quad (\text{A13})$$

For the last part of the lemma we have that

$$[B_{g,x}AB_{g,x}^{-1}, \tilde{X}]_- = \sum_{m,j} \sum_{m',j'} (j' - j)e^{g|j'-x|}e^{-g|j-x|} \langle j, m | A | j', m' \rangle |j, m\rangle \langle j', m' | \quad (\text{A14})$$

but it is easily verified that

$$|(j' - j)e^{g|j'-x|}e^{-g|j-x|}| \leq |j - j'|e^{g|j-j'|} \quad (\text{A15})$$

and hence the result follows by using an analogous calculation as for  $B_{g,x}AB_{g,x}^{-1} - A$ .  $\square$

## Appendix B: Proof of Lemma III.2

To prove this lemma, we will show that there exists a constant  $C$  and a  $g > 0$  so that for any  $x \in \mathbb{R}$  the following estimate holds:

$$\|B_{g,x}P_{\text{qp}}B_{g,x}^{-1}\| \leq C \quad (\text{B1})$$

Proving Eq. (B1) implies the lemma since by definition of the spectral norm:

$$\|A\| = \sup_{\|f\|=\|g\|=1} \langle g | A | f \rangle \quad (\text{B2})$$

Hence, Eq. (B1) implies

$$\begin{aligned} & |\langle j, m | B_{g,x}P_{\text{qp}}B_{g,x}^{-1} | j', m' \rangle| \leq C \\ & \implies e^{g|j-x|}e^{-g|j'-x|} |\langle j, m | P_{\text{qp}} | j', m' \rangle| \leq C. \end{aligned} \quad (\text{B3})$$

Since this holds for any  $x \in \mathbb{R}$  we can choose  $x = j'$  to conclude that

$$|\langle j, m | P_{\text{qp}} | j', m' \rangle| \leq C e^{-g|j-j'|} \quad (\text{B4})$$

which is what we wanted to show.

By the Riesz projection formula, we can express  $P_{\text{qp}}$

$$P_{\text{qp}} = \frac{1}{2\pi i} \int_{\mathcal{C}} (z - H)^{-1} dz \quad (\text{B5})$$

where  $\mathcal{C}$  is a contour in the complex plane which encloses  $\sigma(H) \cap [\Delta, \infty)$ . Note that since  $H$  is bounded,  $\mathcal{C}$  has finite length. We can formally calculate

$$\begin{aligned} B_{g,x}P_{\text{qp}}B_{g,x}^{-1} &= \frac{1}{2\pi i} \int_{\mathcal{C}} B_{g,x}(z - H)^{-1}B_{g,x}^{-1} dz \\ &= \frac{1}{2\pi i} \int_{\mathcal{C}} (B_{g,x}(z - H)B_{g,x}^{-1})^{-1} dz \\ &= \frac{1}{2\pi i} \int_{\mathcal{C}} (z - B_{g,x}HB_{g,x}^{-1})^{-1} dz. \end{aligned} \quad (\text{B6})$$

These formal calculations are justified so long as we can show that the resolvent  $(z - B_{g,x}HB_{g,x}^{-1})^{-1}$  is bounded for all  $z \in \mathcal{C}$ . For any fixed  $z$  we have that

$$\begin{aligned} (z - B_{g,x}HB_{g,x}^{-1})^{-1} &= (z - H - (B_{g,x}HB_{g,x}^{-1} - H))^{-1} \\ &= (z - H)^{-1} \left( \mathbb{1} - (B_{g,x}HB_{g,x}^{-1} - H)(z - H)^{-1} \right)^{-1} \end{aligned} \quad (\text{B7})$$

Hence, if  $z \notin \sigma(H)$  and  $\|(B_{g,x}HB_{g,x}^{-1} - H)(z - H)^{-1}\| < 1$  we can conclude that  $(z - B_{g,x}HB_{g,x}^{-1})^{-1}$  is bounded.

In particular, if we define  $\delta^{-1} := \sup_{z \in \mathcal{C}} \|(z - H)^{-1}\|$  then Lemma A.2 implies for all  $z \in \mathcal{C}$

$$\|(B_{g,x}HB_{g,x}^{-1} - H)(z - H)^{-1}\| \leq 8CD\delta^{-1}g \quad (\text{B8})$$

Hence if  $g < \frac{\delta}{8CD}$ , the above calculation implies for all  $z \in \mathcal{C}$

$$\|(z - B_{g,x}HB_{g,x}^{-1})^{-1}\| \leq \frac{\delta^{-1}}{1 - 8CD\delta^{-1}g}. \quad (\text{B9})$$

This finally implies that

$$\|B_{g,x}P_{\text{qp}}B_{g,x}^{-1}\| \leq \frac{\ell(\mathcal{C})}{2\pi} \frac{\delta^{-1}}{1 - 8CD\delta^{-1}g} \quad (\text{B10})$$

where  $\ell(\mathcal{C})$  is the length of the contour  $\mathcal{C}$  in the complex plane.

**Remark B.1.** From these calculations, we estimate the exponential decay rate of  $P_{\text{qp}}$  is  $O(\delta^{-1})$  (i.e. the decay rate of  $P_{\text{qp}}$  is proportional to the inverse gap of  $H$ ).

## Appendix C: Proof of Theorem III.3

For this proof we will use Lemma III.2 and suppose  $P_{\text{qp}}$  is an exponentially localized operator with rate  $\kappa_{\text{qp}}$  and prefactor  $C_{\text{qp}}$ . We will also make use of the following simple lemma which has appeared in a number of previous works [47–49]

**Lemma C.1.** *Let  $A_1, A_2$  be two bounded operators. If  $A_1$  is positive semidefinite then*

$$\|[A_1, A_2]_-\| \leq \|A_1\| \|A_2\|. \quad (\text{C1})$$

*If both  $A_1$  and  $A_2$  are positive semidefinite then*

$$\|[A_1, A_2]_-\| \leq \frac{1}{2} \|A_1\| \|A_2\|. \quad (\text{C2})$$

*Proof.* Let's first suppose that only  $A_1$  is positive semidefinite. Since  $A_1$  is bounded, we have that  $\sigma(A_1) \subseteq [0, \|A_1\|]$ . Now define the operator  $\tilde{A}_1 := A_1 - \frac{1}{2}\|A_1\|$  and observe that

$$\sigma(\tilde{A}_1) \subseteq \left[ -\frac{1}{2}\|A_1\|, \frac{1}{2}\|A_1\| \right]. \quad (\text{C3})$$

Hence  $\|\tilde{A}_1\| = \frac{1}{2}\|A_1\|$ . Therefore

$$\begin{aligned} \|[A_1, A_2]_-\| &= \|[\tilde{A}_1, A_2]_-\| \\ &\leq 2\|\tilde{A}_1\|\|A_2\| = \|A_1\|\|A_2\|. \end{aligned} \quad (\text{C4})$$

If  $A_2$  is also positive semidefinite, we can replace  $A_2$  with  $\tilde{A}_2 := A_2 - \frac{1}{2}\|A_2\|$  as well to get the second bound.  $\square$

---

### 1. Proof $P_{\text{qp}}\tilde{X}P_{\text{qp}}$ has discrete spectrum

We will prove that  $P_{\text{qp}}\tilde{X}P_{\text{qp}}$  has compact resolvent on range( $P_{\text{qp}}$ ) and hence  $P_{\text{qp}}\tilde{X}P_{\text{qp}}$  only has discrete eigenvalues. In the first step, we show that for sufficiently large  $\alpha > 0$ , the operator  $P_{\text{qp}}\tilde{X}P_{\text{qp}} \pm i\alpha$  has full rank on range( $P_{\text{qp}}$ ). Consider the following expression

$$(P_{\text{qp}}\tilde{X}P_{\text{qp}} \pm i\alpha)P_{\text{qp}}(\tilde{X} \pm i\alpha)^{-1}P_{\text{qp}}. \quad (\text{C5})$$

Note that  $(\tilde{X} \pm i\alpha)^{-1}$  is well defined and  $\|(\tilde{X} \pm i\alpha)^{-1}\| \leq \alpha^{-1}$ . Since  $P_{\text{qp}}$  is a projection we have

$$\begin{aligned} (P_{\text{qp}}\tilde{X}P_{\text{qp}} \pm i\alpha)P_{\text{qp}}(\tilde{X} \pm i\alpha)^{-1}P_{\text{qp}} &= P_{\text{qp}}(\tilde{X} \pm i\alpha)P_{\text{qp}}(\tilde{X} \pm i\alpha)^{-1}P_{\text{qp}} \\ &= P_{\text{qp}}\left(P_{\text{qp}}(\tilde{X} \pm i\alpha) + [\tilde{X} \pm i\alpha, P_{\text{qp}}]_-\right)(\tilde{X} \pm i\alpha)^{-1}P_{\text{qp}} \\ &= P_{\text{qp}} + P_{\text{qp}}[\tilde{X}, P_{\text{qp}}]_-(\tilde{X} \pm i\alpha)^{-1}P_{\text{qp}}. \end{aligned} \quad (\text{C6})$$

Since  $[\tilde{X}, P_{\text{qp}}]_-$  is bounded by Lemma A.2, by choosing  $\alpha$  sufficiently large we can ensure that  $\|[\tilde{X}, P_{\text{qp}}]_-(\tilde{X} \pm i\alpha)^{-1}\| < 1$  which implies that  $(P_{\text{qp}}\tilde{X}P_{\text{qp}} \pm i\alpha)$  is full rank on range( $P_{\text{qp}}$ ) and hence self-adjoint on this domain[50, Theorem VIII.3].

Consequently, we can invert  $(P_{\text{qp}}\tilde{X}P_{\text{qp}} \pm i\alpha)$  and  $P_{\text{qp}} + P_{\text{qp}}[\tilde{X}, P_{\text{qp}}]_-(\tilde{X} \pm i\alpha)^{-1}P_{\text{qp}}$  to get that

$$\begin{aligned} (P_{\text{qp}}\tilde{X}P_{\text{qp}} \pm i\alpha)^{-1} &= P_{\text{qp}}(\tilde{X} \pm i\alpha)^{-1}P_{\text{qp}}\left(P_{\text{qp}} + P_{\text{qp}}[\tilde{X}, P_{\text{qp}}]_-(\tilde{X} \pm i\alpha)^{-1}P_{\text{qp}}\right)^{-1} \\ &= \left(P_{\text{qp}}(\tilde{X} \pm i\alpha)^{-1}\right)\left(P_{\text{qp}} + P_{\text{qp}}[\tilde{X}, P_{\text{qp}}]_-(\tilde{X} \pm i\alpha)^{-1}P_{\text{qp}}\right)^{-1}. \end{aligned} \quad (\text{C7})$$

We now show that the first factor in the final expression is compact. For any integer  $j_0 > 0$  we can write  $P_{\text{qp}}(\tilde{X} \pm i\alpha)^{-1}$  as

$$P_{\text{qp}}(\tilde{X} \pm i\alpha)^{-1} = \left(P_{\text{qp}}\chi(|\tilde{X}| \leq j_0)\right)(\tilde{X} \pm i\alpha)^{-1} + P_{\text{qp}}\left(\chi(|\tilde{X}| > j_0)(\tilde{X} \pm i\alpha)^{-1}\right), \quad (\text{C8})$$

where

$$\chi(|\tilde{X}| \leq j_0) := \sum_{m=1}^D \sum_{|j| \leq j_0} |j, m\rangle \langle j, m| =: \mathbb{1} - \chi(|\tilde{X}| > j_0). \quad (\text{C9})$$


---

But observe that

$$\begin{aligned} \|P_{\text{qp}}\chi(|\tilde{X}| \leq j_0)\|_F^2 &= \sum_{m,j} \sum_{m',|j| \leq j_0} |\langle j, m | P_{\text{qp}} |j', m' \rangle|^2 \\ &\leq 2j_0 D \left( \sup_{j'} \sum_{m,j} |\langle j, m | P_{\text{qp}} |j', m' \rangle|^2 \right) \\ &\leq 2C_{\text{qp}} j_0 D^2 \sum_j e^{-\kappa_{\text{qp}}|j|} < \infty. \end{aligned} \quad (\text{C10})$$

Therefore  $P_{\text{qp}}\chi(|\tilde{X}| \leq j_0)$  is a Hilbert-Schmidt operator and hence compact. By definition

$$\begin{aligned} \|P_{\text{qp}}\chi(|\tilde{X}| > j_0)(\tilde{X} \pm i\alpha)^{-1}\| &\leq \|\chi(|\tilde{X}| > j_0)(\tilde{X} \pm i\alpha)^{-1}\| \\ &\leq (j_0^2 + \alpha^2)^{-1/2}. \end{aligned} \quad (\text{C11})$$

Hence, we have that  $P_{\text{qp}}(\tilde{X} \pm i\alpha)^{-1}$  is the limit of compact operators in the operator norm and hence also compact.

Therefore,  $(P_{\text{qp}}\tilde{X}P_{\text{qp}} \pm i\alpha)^{-1}$  is compact and  $P_{\text{qp}}\tilde{X}P_{\text{qp}}$  has compact resolvent on range  $(P_{\text{qp}})$ .

## 2. Proof $P_{\text{qp}}\tilde{X}P_{\text{qp}}$ has exponentially localized eigenfunctions

For this proof we will introduce notation for step function

$$\chi_{x,b} := \sum_{m=1}^D \sum_{|j-x| \leq b} |j, m\rangle \langle j, m|, \quad (\text{C12})$$

which depends on parameters  $x \in \mathbb{R}$ ,  $b \in \mathbb{R}^+$ . That is  $\chi_{x,b}$  is a ‘‘step’’ of width  $b$  centered at the real number  $x$ . Observe that for any choice of  $x$  or  $b$  the operator  $\chi_{x,b}$  is a positive operator. With this definition, we now proceed with the proof.

Suppose that  $|\phi\rangle \in \text{range}(P_{\text{qp}})$  is an eigenfunction of  $P_{\text{qp}}\tilde{X}P_{\text{qp}}$  with eigenvalue  $x$ . By definition this means

$$P_{\text{qp}}\tilde{X}P_{\text{qp}}|\phi\rangle = x|\phi\rangle \iff P_{\text{qp}}(\tilde{X} - x)P_{\text{qp}}|\phi\rangle = 0. \quad (\text{C13})$$

Let  $b \in \mathbb{R}^+$  be a parameter to be chosen later, adding  $ib\chi_{x,b}|\phi\rangle$  to both sides gives

$$P_{\text{qp}}(\tilde{X} - x + ib\chi_{x,b})P_{\text{qp}}|\phi\rangle = ib\chi_{x,b}|\phi\rangle. \quad (\text{C14})$$

Our basic goal in this proof will be to rewrite Eq. (C14) as

$$|\phi\rangle = \mathcal{L}\chi_{x,b}|\phi\rangle, \quad (\text{C15})$$

where  $\mathcal{L}$  is some linear operator. Once we can show this, we will multiply both sides by  $B_{g,x}$  to get that

$$B_{g,x}|\phi\rangle = B_{g,x}\mathcal{L}\chi_{x,b}|\phi\rangle = (B_{g,x}\mathcal{L}B_{g,x}^{-1})(B_{g,x}\chi_{x,b}|\phi\rangle). \quad (\text{C16})$$

We will then show that for a choice of  $b$  large enough and all  $g$  sufficiently small, there exists a constant  $C$  so that  $\|B_{g,x}\mathcal{L}B_{g,x}^{-1}\| \leq C$ . Since  $\chi_{x,b}$  is a step function we have

$$\|B_{g,x}|\phi\rangle\| \leq Ce^{gb}\|\phi\|, \quad (\text{C17})$$

which immediately implies that

$$|\langle j, m | \phi \rangle| \leq Ce^{gb}e^{-g|j-x|}. \quad (\text{C18})$$

Importantly, the choice of  $b$  depends only on  $P_{\text{qp}}$  and not on  $j$  or  $|\phi\rangle$ . Hence the theorem is proved.

Returning to Eq. (C14), since  $\tilde{X} - x$  has a zero at  $x$  and  $\chi_{x,b}$  is a step function centered at  $x$ , so long as  $b > 0$ , the operator  $(\tilde{X} - x + ib\chi_{x,b})$  is invertible and

$$\|(\tilde{X} - x + ib\chi_{x,b})^{-1}\| \leq b^{-1}. \quad (\text{C19})$$

Therefore, multiplying both sides of Eq. (C14) by  $(\tilde{X} - x + ib\chi_{x,b})^{-1}$  gives

$$(\tilde{X} - x + ib\chi_{x,b})^{-1}P_{\text{qp}}(\tilde{X} - x + ib\chi_{x,b})P_{\text{qp}}|\phi\rangle = i(\tilde{X} - x + ib\chi_{x,b})^{-1}b\chi_{x,b}|\phi\rangle. \quad (\text{C20})$$

Commuting  $P_{\text{qp}}$  and  $(\tilde{X} - x + ib\chi_{x,b})$  on the left hand side to get

$$\left(1 + (\tilde{X} - x + ib\chi_{x,b})^{-1}([P_{\text{qp}}, \tilde{X}]_- + i[P_{\text{qp}}, b\chi_{x,b}]_-)\right)P_{\text{qp}}|\phi\rangle = i(\tilde{X} - x + ib\chi_{x,b})^{-1}b\chi_{x,b}|\phi\rangle. \quad (\text{C21})$$

Upon examining the left hand side a bit more closely, we see that

$$\begin{aligned} & \|(\tilde{X} - x + ib\chi_{x,b})^{-1}([P_{\text{qp}}, \tilde{X}]_- + i[P_{\text{qp}}, b\chi_{x,b}]_-)\| \\ & \leq \|(\tilde{X} - x + ib\chi_{x,b})^{-1}\| \left( \| [P_{\text{qp}}, \tilde{X}]_- \| + b \| [P_{\text{qp}}, b\chi_{x,b}]_- \| \right) \\ & \leq b^{-1} \left( \| [P_{\text{qp}}, \tilde{X}]_- \| + \frac{1}{2}b \right), \end{aligned} \quad (\text{C22})$$

where in the last line we have used C.1. Since

$$\|[P_{\text{qp}}, \tilde{X}]_-\| \leq 8C_{\text{qp}}d\kappa_{\text{qp}}^{-2} \quad (\text{C23})$$

by Lemma A.2, by choosing  $b = 32C_{\text{qp}}d\kappa_{\text{qp}}^{-2}$ , we can ensure that

$$\|(\tilde{X} - x + ib\chi_{x,b})^{-1}([P_{\text{qp}}, \tilde{X}]_- + i[P_{\text{qp}}, b\chi_{x,b}]_-)\| \leq \frac{3}{4}. \quad (\text{C24})$$

In this case, we can invert the operator on the left hand side to get

$$|\phi\rangle = ib \left( \mathbb{1} + (\tilde{X} - x + ib\chi_{x,b})^{-1} ([P_{\text{qp}}, \tilde{X}]_- + i[P_{\text{qp}}, b\chi_{x,b}]_-) \right)^{-1} (\tilde{X} - x + ib\chi_{x,b})^{-1} \chi_{x,b} |\phi\rangle. \quad (\text{C25})$$

We have now recovered Eq. (C15) where

$$\mathcal{L} = ib \left( \mathbb{1} + (\tilde{X} - x + ib\chi_{x,b})^{-1} ([P_{\text{qp}}, \tilde{X}]_- + i[P_{\text{qp}}, b\chi_{x,b}]_-) \right)^{-1} (\tilde{X} - x + ib\chi_{x,b})^{-1}. \quad (\text{C26})$$

Following the argument given above, to complete the proof we only need to show that there exists a constant  $C$  so that  $\|B_{g,x}\mathcal{L}B_{g,x}^{-1}\| \leq C$ . Since  $\tilde{X}$  and  $\chi_{x,b}$  are both diagonal in the position basis we see that

$$B_{g,x}\mathcal{L}B_{g,x}^{-1} = ib \left( \mathbb{1} + (\tilde{X} - x + ib\chi_{x,b})^{-1} ([B_{g,x}P_{\text{qp}}B_{g,x}^{-1}, \tilde{X}]_- + i[B_{g,x}P_{\text{qp}}B_{g,x}^{-1}, b\chi_{x,b}]_-) \right)^{-1} (\tilde{X} - x + ib\chi_{x,b})^{-1}. \quad (\text{C27})$$

Therefore, since  $\|(\tilde{X} - x + ib\chi_{x,b})^{-1}\| \leq b^{-1}$ ,

$$\|B_{g,x}\mathcal{L}B_{g,x}^{-1}\| \leq \left\| \left( \mathbb{1} + (\tilde{X} - x + ib\chi_{x,b})^{-1} ([B_{g,x}P_{\text{qp}}B_{g,x}^{-1}, \tilde{X}]_- + i[B_{g,x}P_{\text{qp}}B_{g,x}^{-1}, b\chi_{x,b}]_-) \right)^{-1} \right\|, \quad (\text{C28})$$

and hence to complete the proof it suffices to show that there exists a choice of  $b$  so that for all  $g$  sufficiently small

$$\|(\tilde{X} - x + ib\chi_{x,b})^{-1} ([B_{g,x}P_{\text{qp}}B_{g,x}^{-1}, \tilde{X}]_- + i[B_{g,x}P_{\text{qp}}B_{g,x}^{-1}, b\chi_{x,b}]_-)\| < 1. \quad (\text{C29})$$

We calculate

$$\begin{aligned} & \|(\tilde{X} - x + ib\chi_{x,b})^{-1} ([B_{g,x}P_{\text{qp}}B_{g,x}^{-1}, \tilde{X}]_- + i[B_{g,x}P_{\text{qp}}B_{g,x}^{-1}, b\chi_{x,b}]_-)\| \\ & \leq b^{-1} \left( \| [B_{g,x}P_{\text{qp}}B_{g,x}^{-1}, \tilde{X}]_- \| + \| [B_{g,x}P_{\text{qp}}B_{g,x}^{-1} - P_{\text{pq}} + P_{\text{pq}}, b\chi_{x,b}]_- \| \right) \\ & \leq b^{-1} \| [B_{g,x}P_{\text{qp}}B_{g,x}^{-1}, \tilde{X}]_- \| + \| [B_{g,x}P_{\text{qp}}B_{g,x}^{-1} - P_{\text{pq}}, \chi_{x,b}]_- \| + \| [P_{\text{pq}}, \chi_{x,b}]_- \| \\ & \leq b^{-1} \| [B_{g,x}P_{\text{qp}}B_{g,x}^{-1}, \tilde{X}]_- \| + \| B_{g,x}P_{\text{qp}}B_{g,x}^{-1} - P_{\text{pq}} \| + \frac{1}{2}, \end{aligned} \quad (\text{C30})$$

where in the last line we have used Lemma C.1 twice. By Lemma A.2,

$$\begin{aligned} & \| [B_{g,x}P_{\text{qp}}B_{g,x}^{-1}, \tilde{X}]_- \| \leq 8C_{\text{qp}}d\kappa_{\text{qp}}^{-2}, \\ & \| B_{g,x}P_{\text{qp}}B_{g,x}^{-1} - P_{\text{pq}} \| \leq 8C_{\text{qp}}d\kappa_{\text{qp}}^{-2}g. \end{aligned} \quad (\text{C31})$$

Therefore, if we choose  $b = 64C_{\text{qp}}D\kappa_{\text{qp}}^{-2}$  and  $g = \kappa_{\text{qp}}^2(64C_{\text{qp}}D)^{-1}$  we conclude that  $\|B_{g,x}\mathcal{L}B_{g,x}^{-1}\| \leq 4$ . Therefore, following the previous argument, we conclude that

$$|\langle j, m | \phi \rangle| \leq 4e \exp \left( -\frac{\kappa_{\text{qp}}^2}{64C_{\text{qp}}D} |j - x| \right). \quad (\text{C32})$$

Note that for the Kitaev chain Hamiltonian, the eigenstates of  $X_{\text{qp}}$  with positive eigenvalues are eigenstates of  $P_{\text{qp}}\tilde{X}P_{\text{qp}}$ , so this finishes the proof of Thm III.3.

#### Appendix D: Average speed of the quasiparticles

In this section, we derive an expression for the average speed of QPs in a superconductor in thermal equilibrium. For simplicity, let us consider a one-dimensional

conductor with dispersion relation  $\xi(k) = \hbar^2 k^2 / 2m$  and with Fermi momentum  $k_F$ . The dispersion relation after the onset of superconductivity is given by  $E(k) = \pm\sqrt{\xi(k)^2 + \Delta^2}$ , where  $\Delta$  is the pairing strength. In the vicinity of  $k_F$ , the energy  $\xi(k)$  can be assumed to be linear, i.e.  $\xi(k) = \hbar v_F(k - k_F)$  for  $|k - k_F| \ll |k_F|$  where  $v_F = \hbar k_F / m$ . Moreover, for  $|k - k_F| \ll \Delta/\hbar v_F$ ,  $E(k)$  can be approximated by

$$E(k) = \Delta + \frac{\hbar^2 v_F^2 (k - k_F)^2}{2\Delta} = \Delta + \frac{\hbar^2 (k - k_F)^2}{2m_{\text{qp}}}, \quad (\text{D1})$$

where  $m_{\text{qp}}$  is the effective mass of the QPs given by

$$\frac{1}{m_{\text{qp}}} = \frac{1}{\hbar^2} \left. \frac{\partial^2 E(k)}{\partial k^2} \right|_{k_F} = \frac{v_F^2}{\Delta}. \quad (\text{D2})$$

The QPs are governed by the Fermi-Dirac distribution and their average occupation is given by [51]

$$\langle n_k \rangle = \frac{1}{1 + e^{\beta E(k)}}. \quad (\text{D3})$$

For  $\beta\Delta \gg 1$ , we have  $\beta E(k) = \beta\Delta + \beta\hbar^2 v_F^2 (k - k_F)^2 / 2\Delta \gg 1$ , and therefore

$$\langle n_k \rangle \approx e^{-\beta E(k)} = e^{-\beta\Delta} e^{-\beta\hbar^2 (k - k_F)^2 / 2m_{\text{qp}}}. \quad (\text{D4})$$

The fraction of QPs with quasi-momentum  $k$  is then given by

$$\frac{\langle n_k \rangle}{\sum_k \langle n_k \rangle} \approx \frac{e^{-\beta \hbar^2 (k - k_F)^2 / 2m_{\text{qp}}}}{\sum_k e^{-\beta \hbar^2 (k - k_F)^2 / 2m_{\text{qp}}}}. \quad (\text{D5})$$

Eq. (D5) reflects the well-known fact that Fermi-Dirac distribution converges to Maxwell-Boltzmann distribution in the limit of low particle density. The distribution

of QPs is thus identical to that of a 1D classical ideal gas, and therefore we can directly use the corresponding formula for the average speed  $\langle |v_{\text{qp}}| \rangle \sim \sqrt{1/\beta m_{\text{qp}}}$ . Substituting the expression for  $m_{\text{qp}}$  in Eq. (D2), we get

$$\langle |v_{\text{qp}}| \rangle \sim v_F \sqrt{1/\beta \Delta} \quad (\text{D6})$$

as desired.